DESIGN & DEVELOPMENT OF

AUTOMATIC NGV NATURAL GAS VEHICLE

REFUELING ROBOT

MOHD NOORSHAHRIL BIN YAAKOB

FACULTY OF ENGINEERING

UNIVERSITY OF MALAYA

KUALA LUMPUR

2013

DESIGN & DEVELOPMENT OF

AUTOMATIC NGV NATURAL GAS VEHICLE

REFUELLING ROBOT

MOHD NOORSHAHRIL BIN YAAKOB

RESEARCH REPORT SUBMITTED IN PARTIAL

FULFILLMENT OF THE REQUIREMENT FOR THE

DEGREE OF MASTER OF ENGINEERING

FACULTY OF ENGINEERING

UNIVERSITY OF MALAYA

KUALA LUMPUR

2013

ABSTRACT

This project paper is aimed to plan and develop an automatic robot for an application of refueling the natural gas vehicle (NGV) with main focus on its trajectory analysis. A KUKA KR16 L6-2 KS robotic arm is chosen to model the kinematics and motion to perform the task, simulated using KUKA SimPro software, taking advantage of its off-line programming capabilities. Two case studies were investigated in the process of modeling, taking into account on the position of fuel filling valve on the vehicle, whether it is horizontally-placed or vertically-placed, where six and five movement points are pre-defined respectively. Also, the point of interests for each case study, namely the end-effector point and the fuel filling point, are pre-defined based on feasible and actual environment. All the points are used for programming by applying the point-to-point (PTP) motion to be loaded into the KR C2 controller. The transformation matrices are derived at each point and also for total robot motion using the forward kinematics approach beside representing the kinematics of each robot joint using Denavit-Hartenberg approach. The angles of each joint at each movement points are calculated using the inverse kinematics approach to provide the significant boundary conditions for determining the overall rotational motion of the robot. Furthermore, the angles calculated are mapped for the robot trajectories at given time using third-order polynomial trajectory planning to give the extended view of the robot orientation and behavior in order to perform the simple task of vehicle refueling.

ABSTRAK

Kertas projek ini dibuat adalah bertujuan untuk merekabentuk dan membangunkan robot automatik dalam aplikasi pengisian minyak untuk kenderaan yang menggunakan sumber gas asli dengan penekanan diberikan untuk analisa trajektori. Robot KUKA KR16 L6-2 dipilih utuk menghasilkan pergerakan dan kinematik untuk aplikasi yang tersebut di atas, dan akan disimulasikan menggunakan perisian KUKA SimPro kerana ia berupaya melaksanakan pengaturcaraan walaupun secara luar talian. Dua situasi disiasat semasa proses pembentukan dengan mengambilkira kedudukan injap pemasukan minyak kenderaan yang terbabit, sama ada terletak secara melintang atau menegak, yang mana enam dan lima titik pergerakan ditentudahulukan bagi setiap situasi tersebut. Titik kedudukan muncung pengisi minyak dan injap pemasukan juga ditentudahulukan berdasarkan keadaan sebenar dan boleh dilaksanakan. Semua titik tersebut digunakan untuk pengaturcaraan dengan pergerakan titik-ke-titik (PTP) yang dimasukkan ke dalam alat kawalan KR C2. Matriks transformasi akan diperolehi menggunakan pendekatan "forward kinematics" di samping pendekatan "Denavit-Hartenberg" untuk mewakili setiap paksi robot. Sudut-sudut dikira pada setiap paksi robot dan titik menggunakan pendekatan "inverse kinematics" untuk menunjukkan pergerakan rotasi robot secara keseluruhan. Akhir sekali, pendekatan "third-order polynomial " digunakan untuk menunjukkan trajektori dan orientasi robot dalam pelaksanaan tugas untuk pengisian minyak kenderaan.

ACKNOWLEDGEMENT

Firstly, thanks to God Almighty Allah S.W.T. who has given me the opportunity and time to carry out this research and accomplish the report in order to complete the Master of Engineering degree in University of Malaya. The highest acknowledgement also reserved for my project supervisor, Dr. Mahidzal Dahari who has been giving a lot of guidance and coaching in robotics field towards producing a high-impact research. Without his assistance, it would be very difficult for the theories to be understood and analysis to be done successfully.

Also special thanks for my colleagues in Mechatronics Engineering, Mr. Hasan Firdaus and Mr. Syamsuzzaman who has been working together and sharing their knowledge in this project. Lastly, gratitude towards my family members who has been supporting me all along my study and also other people who has involved directly or indirectly in the completion of this project.

TABLE OF CONTENTS

ABSTRACT ii

ABSTRAK iii

ACKNOWLEDGEMENT iv

LIST OF FIGURES vii

LIST OF TABLES viii

LIST OF SYMBOLS AND ABBREVIATIONS ix

1.0 Introduction 1

1.1 Importance of Study 5

1.2 Problem Statement and Objectives 6

1.3 Scope and Limitations of Study 6

2.0 Literature Review 8

2.1 Summary 11

3.0 Project Methodology 12

3.1 Environment Layout 16

3.1.1 Setup and Layout for Case Study 1: Horizontal Valve 17

3.1.2 Setup and Layout for Case Study 2: Vertical Valve 19

3.2 Robot and Controller Used 21

3.3 Denavit-Hartenberg Representation 22

3.4 Forward Kinematics Analysis 25

3.4.1 Case Study 1: Horizontal Fuel-Filling Valve Position 25

3.4.1.1 Positioning at P1 25

3.4.1.2 Analysis at P2 26

3.4.1.3 Analysis at P3 26

3.4.1.4 Analysis at P4 27

3.4.1.5 Analysis at P5 27

3.4.1.6 Analysis at P6 28
3.4.2 Case Study 2: Vertical Fuel-Filling Valve Position 28
3.4.2.1 Positioning at P1 28
3.4.2.2 Analysis at P2 29
3.4.2.3 Analysis at P3 29
3.4.2.4 Analysis at P4 30
3.4.2.5 Analysis at P5 30
3.5 Inverse Kinematics Analysis 31
3.6 Trajectory Planning 33
3.7 Summary 34
4.0 Results and Discussion 35
4.1 Forward and Inverse Kinematics of the Robot 35
4.2 Trajectory Analysis for Case Study 1 - Horizontal Valve 40
4.3 Trajectory Analysis for Case Study 2 - Vertical Valve 46
4.4 Summary 52
5.0 Conclusion 53
5.1 Recommendations 53
APPENDIX 54
BIBLIOGRAPHY 56

LIST OF FIGURES

Figure 1.1: General Diagram of Natural Gas Vehicle (NGV) 2

Figure 1.2: Normal type of cylinder fitted into NGV 3

Figure 1.3: NGV Stations in Phoenix Sky Harbor International Airport, US 4

Figure 1.4: Honda Civic GX, one of NGV in the world 4

Figure 2.1: D-H Convention and Notation for Six-Joint Manipulators 9

Figure 2.2: Difference Between Path and Trajectory 10

Figure 3.1: Summary flowchart of project methodology 12

Figure 3.2: Horizontally-placed fuel filling valve on a car 13

Figure 3.3: Vertically-placed fuel-filling valve on a bus 13

Figure 3.4: Natural Gas Fuelling System, courtesy of Greenfield 14

Figure 3.5: Diagram of Fast-Fill Refuelling Station 15

Figure 3.6: Diagram of Slow-Fill Refuelling Station 15

Figure 3.7: Top and front view of setup layout - Case Study 1 17

Figure 3.8: Top and front view of setup layout - Case Study 2 19

Figure 3.9: KUKA KR16 L6-2 KS robotic arm 21

Figure 3.10: Representation of Axes at Each Joint 22

Figure 4.1: Model of six serial links of the robot 36

Figure 4.2: Simulation Model for Case Study 1 Using MATLAB 38

Figure 4.3: Simulation Model for Case Study 2 Using MATLAB 39

Figure 4.4: Joint 1 Angle and Velocity Graphs - Case Study 1 40

Figure 4.4: Joint 2 Angle and Velocity Graphs - Case Study 1 41

Figure 4.6: Joint 3 Angle and Velocity Graphs - Case Study 1 42

Figure 4.7: Joint 5 Angle and Velocity Graphs - Case Study 1 43

Figure 4.8: Joint 6 Angle and Velocity Graphs - Case Study 1 44

Figure 4.9: Overall Joint Angle and Velocity Graphs - Case Study 1 45

Figure 4.10: Joint 1 Angle and Velocity Graphs - Case Study 2 46

Figure 4.11: Joint 2 Angle and Velocity Graphs - Case Study 2 47

Figure 4.12: Joint 3 Angle and Velocity Graphs - Case Study 2 48

Figure 4.13: Joint 5 Angle and Velocity Graphs - Case Study 2 49

Figure 4.14: Joint 6 Angle and Velocity Graphs - Case Study 2 50

Figure 4.15: Overall Joint Angle and Velocity Graphs - Case Study 2 51

LIST OF TABLES

Table 3.1: Parameter Table of Robot Links and Joints 23

Table 3.2: Joint Angles for Case Study 1 (Horizontal Valve) 32

Table 3.3: Joint Angles for Case Study 2 (Vertical Valve) 32

Table 4.1: Joint 1 Angles and Velocities Equations - Case Study 1 40

Table 4.2: Joint 2 Angles and Velocities Equations - Case Study 1 41

Table 4.3: Joint 3 Angles and Velocities Equations - Case Study 1 42

Table 4.4: Joint 5 Angles and Velocities Equations - Case Study 1 43

Table 4.5: Joint 6 Angles and Velocities Equations - Case Study 1 44

Table 4.6: Joint 1 Angles and Velocities Equations - Case Study 2 46

Table 4.7: Joint 2 Angles and Velocities Equations - Case Study 2 47

Table 4.8: Joint 3 Angles and Velocities Equations - Case Study 2 48

Table 4.9: Joint 5 Angles and Velocities Equations - Case Study 2 49

Table 4.10: Joint 6 Angles and Velocities Equations - Case Study 2 50

LIST OF SYMBOLS AND ABBREVIATIONS

DOF	degrees-of-freedom
PTP	point-to-point
A_{n+1}	homogeneous transformation
θ_n	joint angle
d_n	link offset
a_n	link length
α_n	link twist
C_i	cosine θ_i
S_i	sine θ_i
C_{ij}	cosine $(\theta_i + \theta_j)$
S_{ij}	sine $(\theta_i + \theta_j)$
${}^{i}T_j$	transformation matrix from i to j
θ_i	initial joint angle
θ_f	final joint angle
$\dot{\theta}_i$	initial joint velocity
$\dot{\theta}_f$	final joint velocity
C_n	polynomial equation constants
σ	joint type
rad	radian
deg or °	degrees
sec	seconds

1.0 Introduction

In the yesteryears, most of works in heavy duty industry, such as factories, construction and manufacturing, involved lots of manpower to control and perform the tasks. Often problems occurred when human has their own limit, as time constraint to finish the works or mistakes in some stages in order to produce a good product. Then an issue comes when human is deemed 'unfit' to be a worker because of disadvantages of manpower. Other issue includes the shortage of labour power in this world characterized by dwindling birth-rate and aging population, thus creating huge problem in industry.

Therefore, few years back, lots of researches and development in robotics have been done, leading by big power country, such as Japan, United States of America (USA) and Russia. Starting from scratch, those countries are regarded as "big power of robot" as they produce more than half of industrial robot in this world and still researching to produce better robots. For developing countries like Malaysia, Singapore and India, the implementation of robots in industry still in intermediate level might be because of financial constraint and late to cope with new technologies.

Meanwhile, a natural gas vehicle or NGV is a vehicle that uses compressed natural gas (CNG) or liquefied natural gas (LNG) as a less-polluted option to other fossil fuels [11]. Vehicles can operate on this natural gases, either through the use of specifically designed engines for natural gas or by modifying an engine designed to run on gasoline or diesel. NGV can be dedicated to natural gas as a fuel source, or they can be bi-fuel, running on either natural gas or gasoline or natural gas or diesel. Because most natural gas engines are spark-ignited, the usual bi-fuel pairing is natural gas and gasoline. Natural gas engine technologies can differ in the method used to ignite the fuel

in the engine cylinders, the air-fuel ratio, the compression ratio, and the resulting performance and emissions capabilities [9].

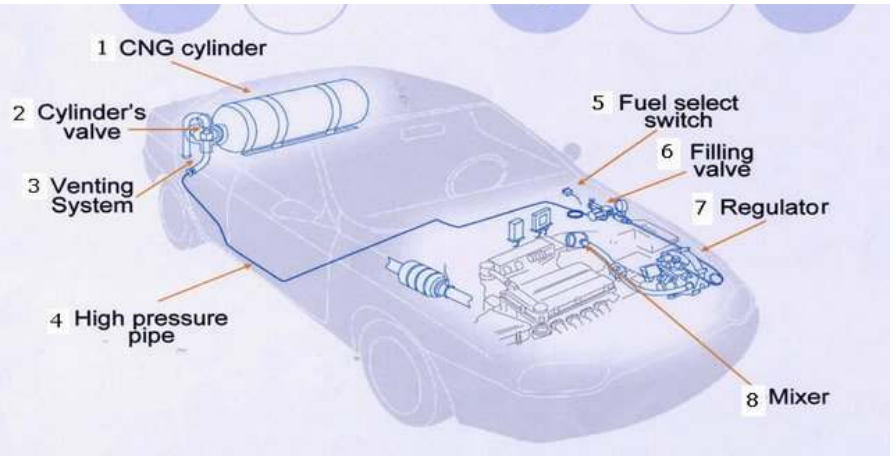

Figure 1.1: General Diagram of Natural Gas Vehicle (NGV)

Natural gas has a high octane rating, which allows an increase in power in spark-ignition engines. However, natural gas occupies a larger volume in the engine cylinder than liquid fuels, reducing the number of oxygen molecules with the sharing of air in the cylinder, which reduces power. The net effect on natural gas power versus gasoline is relatively neutral. Because natural gas is a gaseous fuel at atmospheric pressure and occupies a considerably larger storage volume per unit of energy than refined petroleum liquids, it is stored aboard the vehicle as either a compressed gas or a liquid. The storage requirements are still much greater than those for refined petroleum products, which increases vehicle weight and tends to reduce fuel economy. For vehicles currently use gasoline as their fuel source need to be modified for them to utilize the natural gases. The tanks can be made entirely from metal and they are typically composed of lighter weight metal liners reinforced by a wrap of composite fibre material. Since the gas need be filled into cylinders, these cylinders are usually placed in the vehicle's trunk, reducing the space available for other uses. This issue can be resolved by installing the tanks under the body of the vehicle by the factory itself, and giving the space back in the trunk.

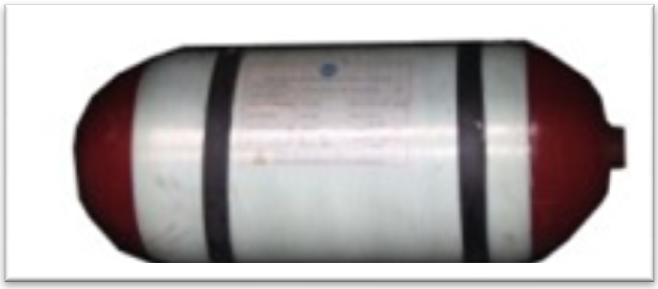

Figure 1.2: Normal type of cylinder fitted into NGV

Currently, there are more initiatives from vehicle manufacturers around the world to produce CNG-powered vehicles as in United States, United Kingdom, Japan, Russia, China, just to name a few. Despite the advantages in cleaner and cheaper fuel substitute, the use of natural gas vehicles encounters several limitations, such as fuel storage and infrastructure available for delivery and distribution at fuelling stations. There is still lack of numbers in gas stations that could offer the distribution of NGV due to small community who are using the natural gas as a source for their vehicle and also because of high investment cost.

NGVs and their respective fuelling systems must meet stringent industry and government standards for compression, storage, and fuelling. They are designed to perform safely during both normal operations and crashes. Nozzles and vehicle receptacles are designed to keep fuel from escaping during refuelling by locking together to form a sealed system. In case of a vehicle fire or impact, a pressure-relief device in the tank allows for controlled venting of the gas so pressure is not built up in the tank. Storage tanks must be regularly inspected for deterioration or damage.

Figure 1.3: NGV Stations in Phoenix Sky Harbor International Airport, United States

But in the years to come, it is expected for the NGV to be slowly coming into the fray. Honda had already produced their own natural gas powered vehicle in their Honda Civic GX in United States [7]. The other factor that could be taken into consideration is to reduce the greenhouse gas effect, the natural gas has proven to be emitting less carbon monoxide and dioxide, non-methane organic gas and nitrogen oxides. With this development, it is not impossible if the demand will increase in immediate effect that will make the gas stations race to provide the service to customers who are seeking cheaper alternative of fuel.

Figure 1.4: Honda Civic GX, one of NGV in the world

Currently, all land vehicles which are using natural gas normally use manual method to fill in the gas. But what if there is shortage of labour at that place and there is no one knows on how to fill in the gas? This is where the robots could come in handy to perform the task. Beside the manpower shortage issue could be discarded, it is also safer for the robot and its automation to involve with the process due to more and more intelligence robot is developed in the worldwide. But in this gas station field there could be found none who adopted robot as their helper except for gas filling of fleets & flights. Therefore, it is an encouragement to develop a robotic system which is not widely used yet but might become a hit in years to come.

1.1 Importance of Study

It has to be admitted that robots have been playing a major role in industrial and automation worldwide whether it is highly-dependent or assisting human to perform the job. Meanwhile in the category of service robots, it is continually growing due to extensive research done by researchers to take advantage of the robots' capability and flexibility towards adapting in its environment. However there are still a lot of field not being explored by researchers that might have opportunity for improvement. Therefore for this project, by combining the industrial robotics and fuel-filling service, development of robot to perform a specific task in filling the NGV application is proposed and analysed on its feasibility. This study may be the kick-start for other research in improving the gas station service, such as gasoline filling, vehicle cleaning or even maintaining the tyre pressure using the robots. The findings in this study could also be used for improvement in future project.

1.2 Problem Statement and Objectives

The motivation behind this project is the opportunity to expand the implementation of robotics to service provider field, for which this paper is initiating on the designing and developing the automatic NGV refuelling robot. Small steps should be taken for reaching major achievement in successfully build the robot. Therefore, in this initial stage, the focus will be on the robot kinematic while producing the trajectory analysis to show the feasibility of the proposal towards performing the task. Taking similarity in the painting robot system, the industrial robot with six degrees-of-freedom (DOF) incorporates along fixed path and pre-determined conditions with the end-effector to be the fuel nozzle.

This research project will therefore seek to explore and investigate on the following:

- To identify the environment where the robot could perform the task of NGV refuelling application.
- To simulate the robot based on the environment identified.
- To identify the kinematics modelling solutions of the robot.
- To evaluate the robot's trajectory and orientation.

1.3 Scope and Limitations of Study

This project paper will only focus on the modelling of the 6-DOF robot to perform the task of refuelling the NGV considering the actual environment at the gas filling station, where the movement points have been already fixed from the simulation done. The theories of forward and inverse kinematics together will appropriate representation of 6-DOF robot will be used extensively in this paper. Meanwhile, the

design of the end-effector and the sensor system will not be discussed in this paper yet because the main concern is the capability and feasibility of robot to accomplish the task first. Also, because of current vehicle system does not have specific mechanism to open the fuel flap and cap automatically, it will only consider on the condition that the said items already opened by the time the robot to perform its task and eliminating the possible restrictions.

2.0 Literature Review

Up until now, people lives in the world of robots, as they assist people mostly in construction and manufacturing industries. Robots are built to perform tasks by equipping them with sensors and effectors [17]. Generally there are two types of robots used, the first one is the industrial type where the robots are involved in product manufacturing and its auxiliaries, while the other one is service robot which it is used to provide help for human to perform job such as in hazardous and unachievable condition in human sense. Whereas, an industrial robot could also perform as service robot which is loosely named as industrial service robot such in application of dismantling nuclear power stations or examining welding or painting work on vehicles [15]. Nowadays, this robot type is growing exponentially due to conscience of the service provider and also because of the reasons of saving labour cost and working in non-ergonomic environment. The application of industrial service robot mostly depends on what the end-effector is, for example of welding, painting and machining.

Several theories, calculations and considerations need to be taken into account in order to design and develop a robot with some specific application, which are kinematics and dynamics analysis, control system, sensory system and actuation. In the initial stage, the kinematics modelling is very essential to provide solution for robot orientation. There are lots of researches related to these have been done, such as Balkan *et al.* [16] who dealt with forward and inverse kinematics to carry out modelling of six joint industrial robots. The robot has been represented using Denavit-Hartenberg convention [8] as per Figure 2.1 which the paper emphasized on parameterized joint variable (PJV) method where the robots have been classified into main groups and sub-groups. The main groups are based on rotation matrices of end-effector and

characterized by the twist angles, while the sub-groups are based on point positions of the wrist and characterized by link lengths and offsets.

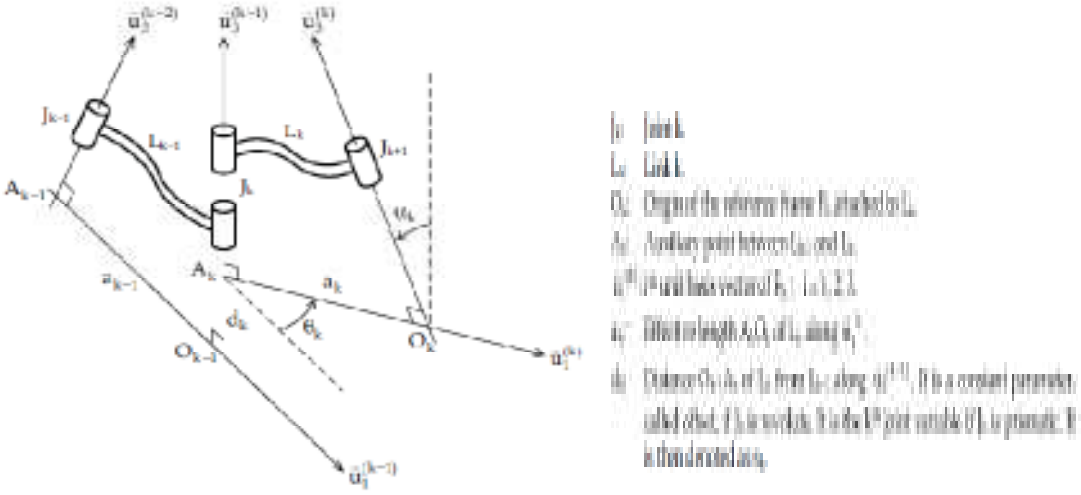

Figure 2.1: D-H Convention and Notation for Six-Joint Manipulators [16]

Other notable research on the kinematics is Kucuk and Bingul (2006) who performs calculations of forward and inverse kinematics solution of robot with degree of freedom ranging from 3 to 6 to show the complexity of each [14]. Beside that there are also researches on kinematics analysis with application such as welding process [10], casing oscillator [20] and spherical parallel manipulators [2].

The main focus of this paper is the analysis of trajectory planning of the robot performing a specific task. Trajectory is a little different from path, in the sense of which, path is the geometrical description of the set of the desired point in the task space while trajectory is the path and time law required to follow it, from the starting to the end point [4,13]. When it is not important to follow a specific path, the trajectory is usually planned in joint-space, implementing a simple point-to-point (PTP) or linear path, while the time law is constrained by the motor maximum velocity and acceleration values [4]. Usually the PTP trajectory in the joint space is obtained by implementing

linear combination of the initial and final values as per Eq. 2.1 where q_0 and q_f are initial and final values respectively.

$$\pi'(q(t)) = (1 - s(t))q_0 + s(t)q_f = q_0 + s(t)\Delta q \quad \text{(Eq. 2.1)}$$

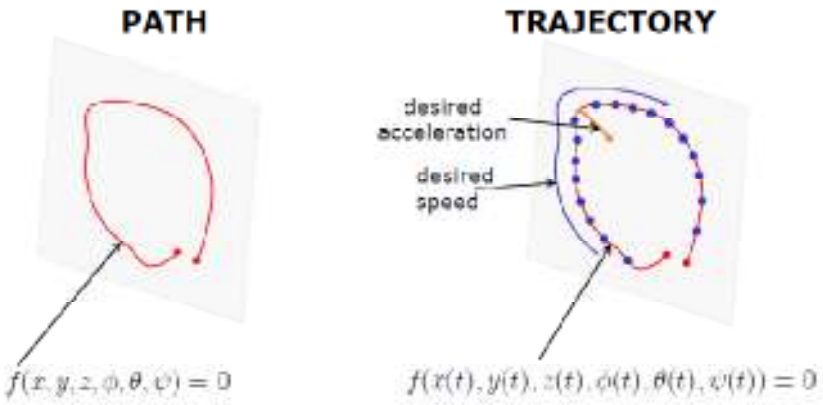

Figure 2.2: Difference Between Path and Trajectory [4]

Other important research regarding the trajectory planning is the application in meal assist robot considering spilling avoidance [19] and measurement with linear inertial sensors [1]. Both papers provide extensive analysis for the trajectory resulted from the application.

Meanwhile for the application of natural gas vehicle refuelling, currently the only system that available is for large type of vehicle such as flights and fleets refuelling system. There is also a breakthrough in robot is used for refuelling satellites in space [5]. The robot known as Special Purpose Dextrous Manipulator or Dextre is performing its robotic refuelling mission which shows that it is not impossible to be done.

2.1 Summary

Based on the reviews of research paper that relates to this project paper, it could be found that a lot of study have been conducted for analysis of kinematics and trajectory planning for robot, with the robot type varied from 3-DOF to 6-DOF. Different methods and algorithms have been studied and proposed to find the absolute solution in determining the orientation, velocity and acceleration of the robot. The methods are investigated thoroughly to ensure the suitable application for this project. Meanwhile in the application of NGV refuelling robot, seems like it is still yet explored by researchers due to low usage of natural gases worldwide.

3.0 Project Methodology

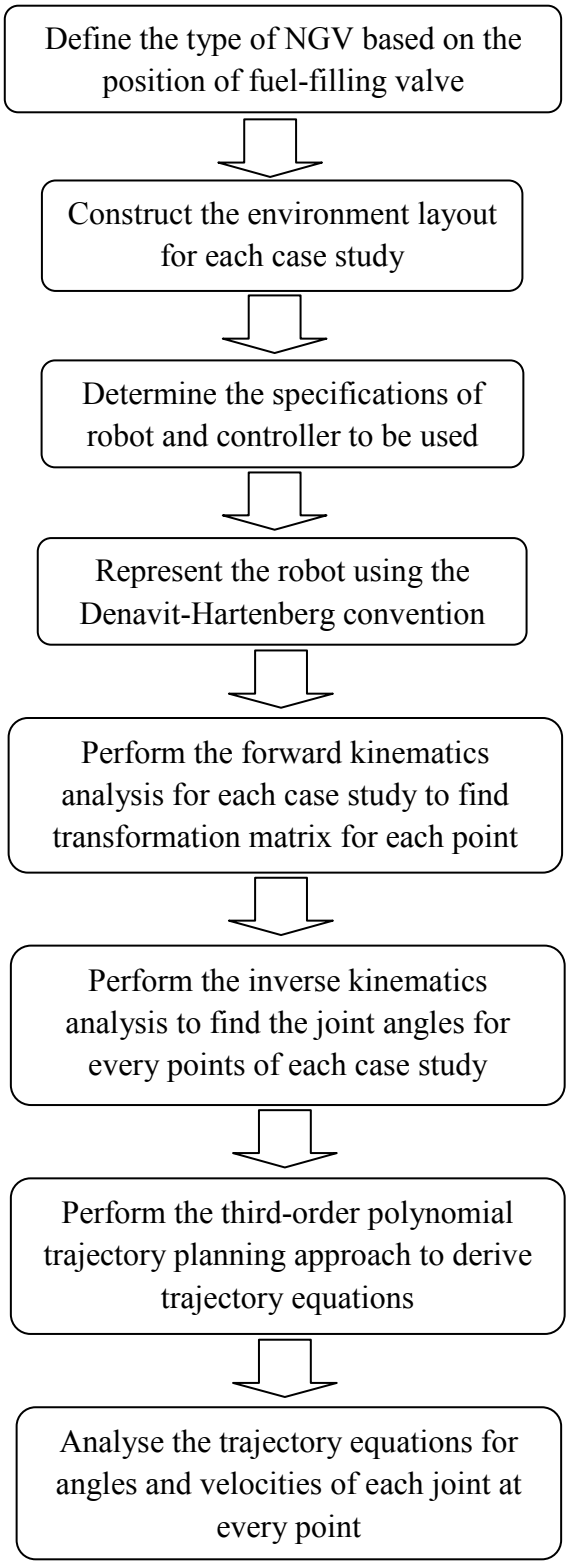

Figure 3.1: Summary flowchart of project methodology

The primary issue that needs to be clarified first is the vehicle type that uses the natural gas and how the refuelling is done at the gas station. Based on observation, there are two types of NGV in the world depending on the position of fuel-filling valve which is horizontally-placed or vertically-placed. For instance, the horizontally-placed valve is used mostly for personal cars and taxis, where the valve is situated under the bonnet in the engine room. Meanwhile the vertically-placed valve is used for bigger vehicle such as vans and buses, which the tank capacity is bigger due to bigger size compared to cars. For this type, the valve is mostly situated on the left or right side of the vehicle, in a similar position of petrol or diesel filling flap.

Figure 3.2: Horizontally-placed fuel filling valve on a car [3]

Figure 3.3: Vertically-placed fuel-filling valve on a bus [12]

Refuelling activity at the station is normally done by station worker or the driver themselves. The refuelling stations could be divided into two distinct categories, fast-fill and slow-fill. Transit facilities such as buses and taxis, almost exclusively use fast-fill stations, although some of their smaller vehicles may also use slow-fill method. In a fast-fill transit bus facilities, compressed gas is stored in a bank of buffer tanks, which are used to help in meeting the initial fuelling demands. The compressors can also bypass the buffer tanks to fuel the vehicles directly. The compressed gas from the buffer tanks or from the compressors is channelled to the dispenser which measures and controls fuel transfer from the dispenser to the vehicle. From the dispenser, which resembles a gasoline dispenser, natural gas is delivered to the vehicle through a semi-flexible, high-pressure hose, which is permanently connected to a nozzle. The open end of the nozzle is designed to fit firmly into a receptacle on the vehicle. The nozzles used for heavy duty, fast-fill fuelling use a valve designed to depressurize the nozzle. In some cases, the valves are sequential dual-action devices, which, after depressurization, also decouple the nozzle from the receptacle. The depressurized gas is channelled through a thin, high-pressure hose to the low-pressure side of the system and is thus recovered.

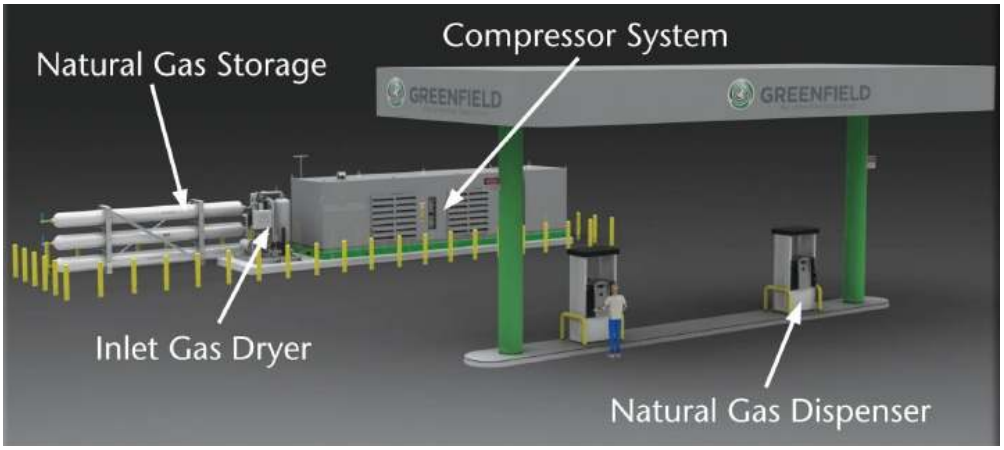

Figure 3.4: Natural Gas Fuelling System, courtesy of Greenfield [6]

In general, when flow is initiated, CNG is pushed from the high-pressure (generally at 4,500 psi) buffer tanks into the onboard cylinders. As the pressure in the buffer tanks drops, the compressors automatically come on. The systems are designed to completely refuel vehicles in timeframes that are comparable (3 to 15 min) to those of gasoline or diesel-fuelled vehicles. Thus, traffic flows at facilities are similar to the flows associated with conventionally fuelled vehicles [18].

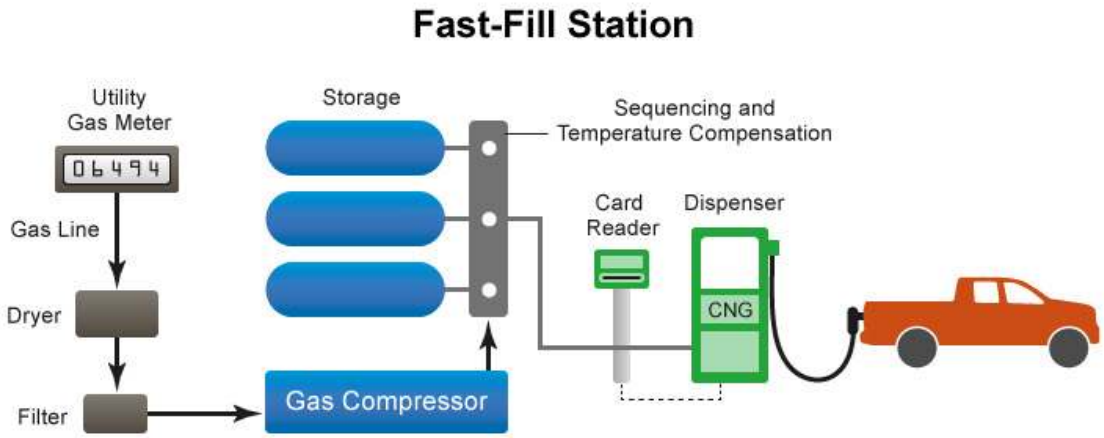

Figure 3.5: Diagram of Fast-Fill Refuelling Station [6]

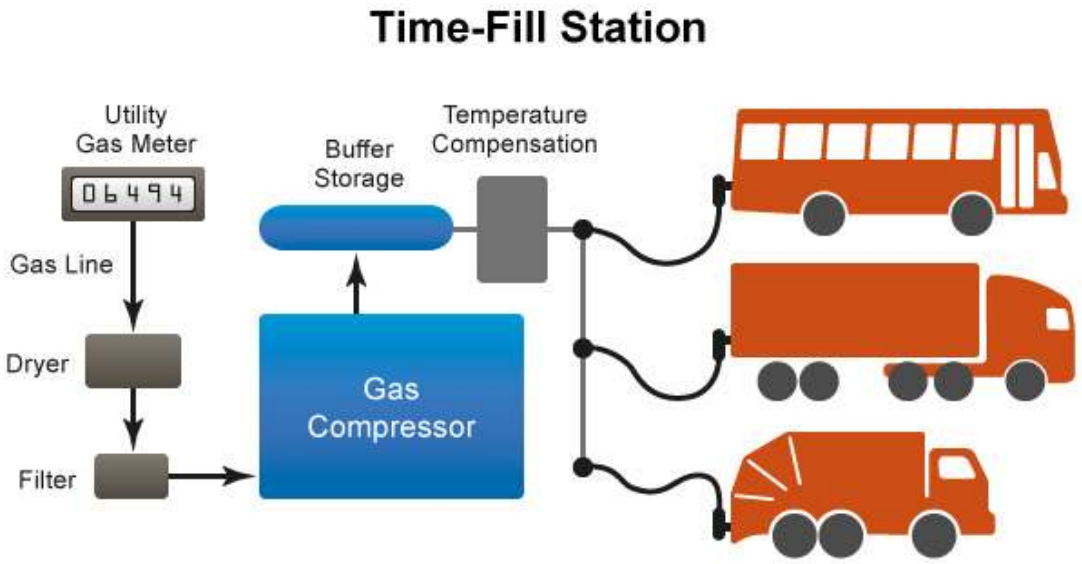

Figure 3.6: Diagram of Slow-Fill Refuelling Station [6]

Meanwhile, slow-fill stations are designed to refuel vehicles in several hours or overnight. Therefore, facilities must be designed to include nozzles at normal parking spaces. Typically, the filling is directly from the compressor output. The compressors are high-pressure compressors with capacity appropriate for the number of nozzles. Dispensers with large numbers of nozzles are at slow-fill stations, where multiple vehicles are fuelled simultaneously. Therefore, for this project those two cases discussed above are taken into investigation on how the robot path will be constructed to fill in the gas.

3.1 Environment Layout

The layout of the position of robot and vehicle is mapped as per actual and feasible environment at the gas station, where the distance between the robot and the vehicle is set to 0.8-meter in order to avoid the collision, which also barely represent current situation when filling the fuel into the vehicle. There will also be a station need to be erected for the purpose of purging or cleaning after every round of fuel filling is performed. Another issue that is assumed for this project is the cap of the valve already been opened to start the robot process, because currently there is no mechanism on the vehicle to automatically open the valve cap as more research need to be done to solve this issue. Therefore the setup and layout for each case study is determined.

3.1.1 Setup and Layout for Case Study 1: Horizontal Valve

For this case, a dimension of an average car is considered, which found to be around 5m in length, 2.3m in width and 1.7m in height. The filling valve is normally situated 50mm from the edge of the car and in 50mm deep. The car is positioned so that it is still inside the reach of the robot which is around 1.8m. The purging and cleaning station is situated 0.8m from the robot and 0.72m above the ground. The top view and front view of the setup is depicted in Figure 3.7.

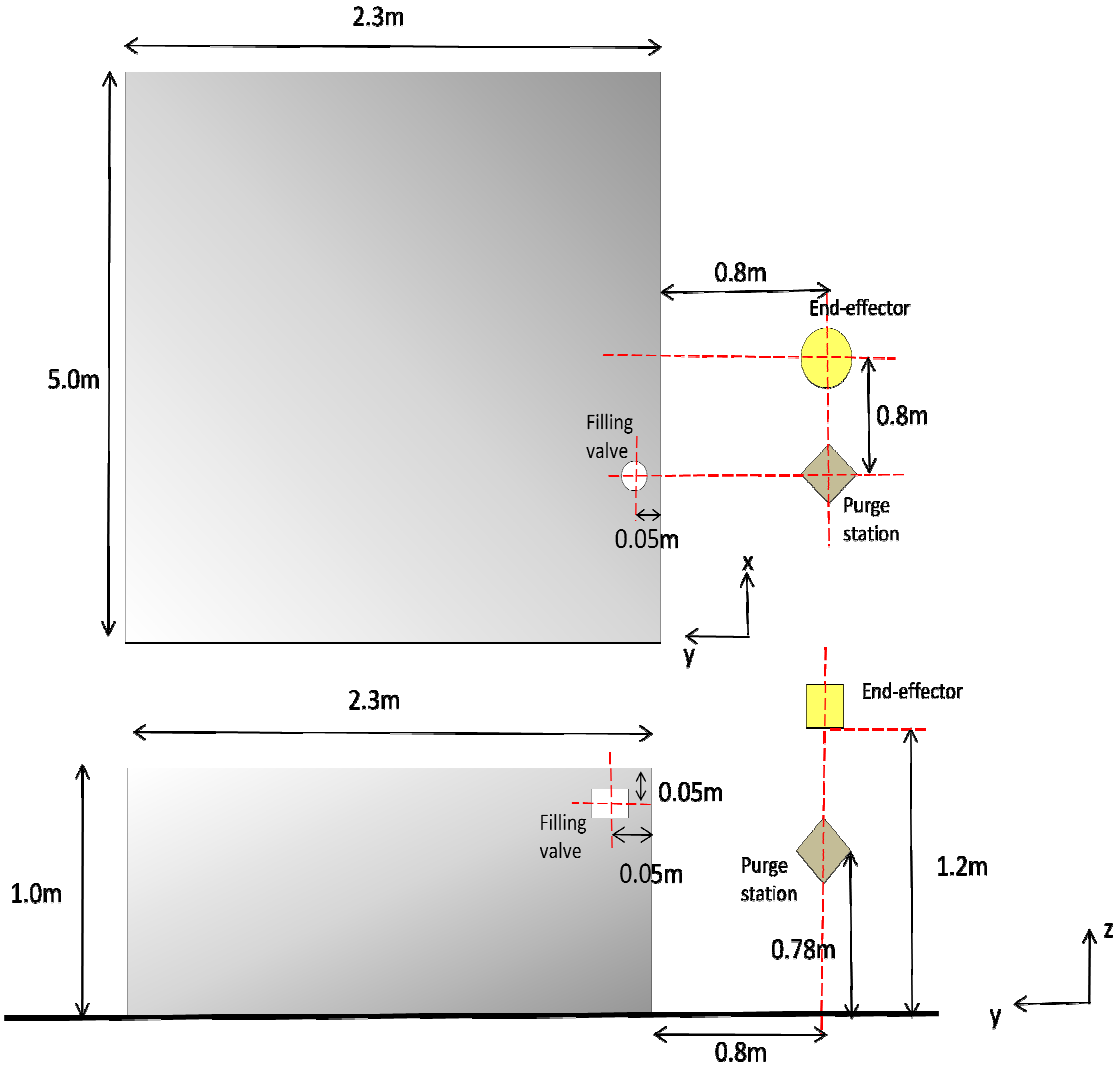

Figure 3.7: Top and front view of setup layout - Case Study 1

In order to perform the task of refuelling, six movement points are fixed which are from point 1 to 6. Point 1, P1, is the starting point of the end-effector is set at -1.13m in x-axis, 0.7m in y-axis and 0.2m in z-axis from the base of the robot. Then it will move to Point 2, P2, at 0.33m along x-axis, 0.3m along y-axis and -0.5m along z-axis, as the robot approaching the car. After that it moves to point 3, P3, at 0.05 along y-axis, approaching the top of the valve, then go down along z-axis by 0.05m to point 4, P4, where the nozzle will snap to the valve. The fuel filling will start at this point and the time taken is depended on the pumping ability at the station. After the filling completed, it moves to point 5, P5, moving 0.07m along z-axis, releasing from the valve. Then the end-effector will stop at point 6, P6, the purging station position.

3.1.2 Setup and Layout for Case Study 2: Vertical Valve

For this case, a dimension of an average bus is considered, which found to be around 14m in length, 3m in width and 9m in height. The filling valve is normally situated 50mm from the fuel flap. The bus is positioned so that it is still inside the reach of the robot as per previous case. The starting point of the end-effector is also the same for both cases. The top view and front view of the setup is depicted in Figure 3.8.

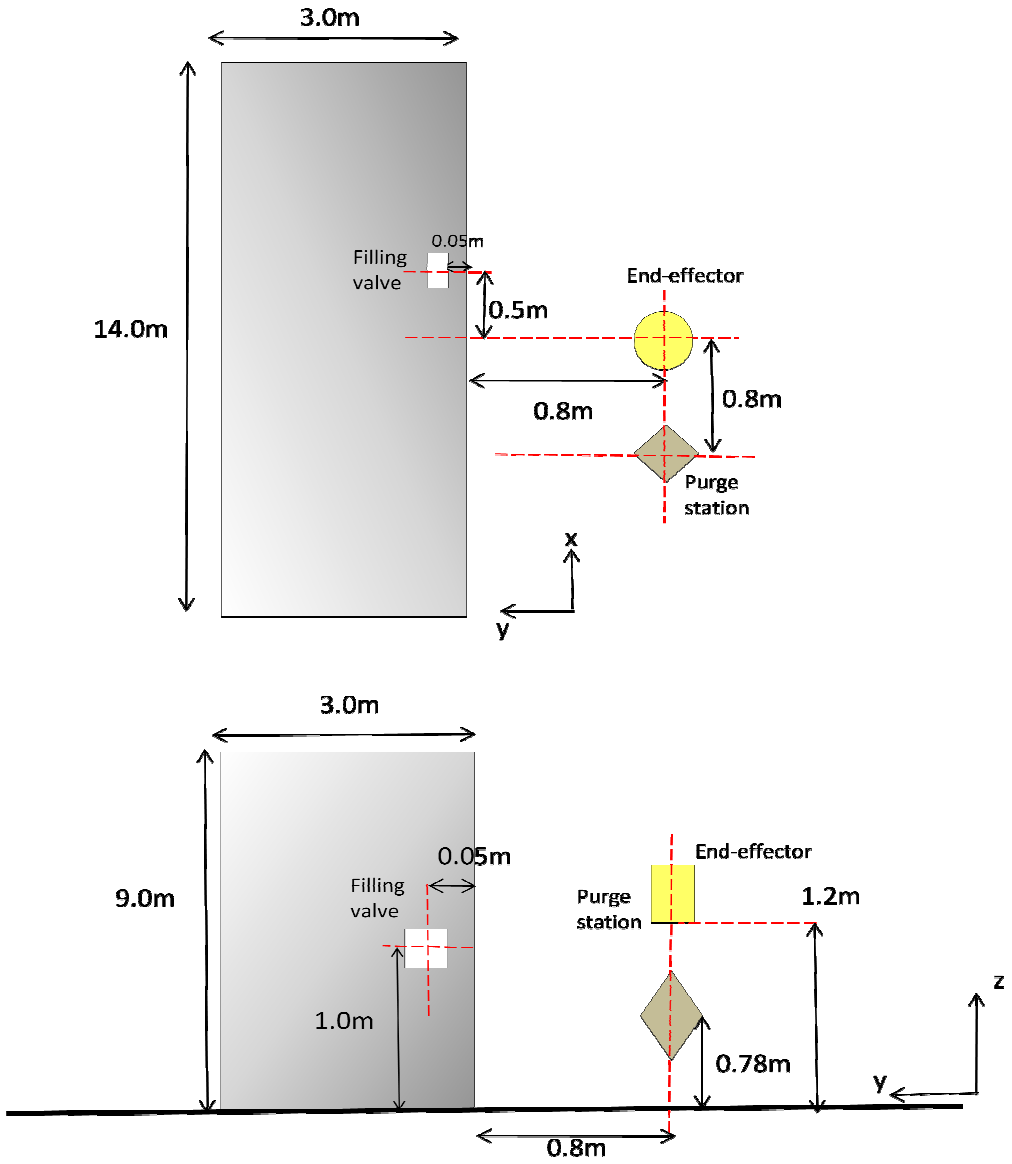

Figure 3.8: Top and front view of setup layout - Case Study 2

To perform the task of refuelling for this case, five movement points are fixed which are from point 1 to 5. Point 1, P1, is the starting point of the end-effector is set at -1.13m in x-axis, 0.7m in y-axis and 0.2m in z-axis from the base of the robot. Then it will move to Point 2, P2, at 1.73m along x-axis, 0.45m along y-axis and -0.5m along z-axis, as the robot approaching the bus. After that it moves to point 3, P3, probe along y-axis by 0.05m where the nozzle will snap to the valve. The fuel filling will start at this point and the time taken is depended on the pumping ability at the station. Then it release the valve to point 4, P4, at -0.1m along y-axis and -0.05m along z-axis. Then, it moves to point 5, P5, moving -1.4m along x-axis, -1.1m along y-axis and 0.07m along z-axis, to the purging station position.

3.2 Robot and Controller Used

For this research purpose, the robot to be used is determined from various type of KUKA robot available. The main characteristics for the application of refuelling robot are low payload with high accuracy and reach because the robot does not need to carry much weight except for the fuel weight. The high accuracy is needed due to the nature of repeatability activity during refuelling process, which could affect the performance of the task accomplishment. Therefore, KUKA KR16 L6-2 KS robotic arm as in Figure 3.9 is chosen to model the kinematics and motion to perform the task as it has the highest reach capability in its class of low payload robot, which is around 2-meter. With a payload in the range of 6kg to 10kg coupled with high reach, it is just a perfect robot to do the job. Another consideration when choosing this robot is the similarity application for painting robot with the intended task of refuelling system for this project.

Figure 3.9: KUKA KR16 L6-2 KS robotic arm

For this type of robot, the controller used is KR C2 developed by KUKA Robotics GmbH which is the standard controller used for other KUKA robot such as KR30 and KR30 JET. In this project, the controller programming is simulated using KUKA SimPro software, taking advantage of its off-line programming capabilities.

3.3 Denavit-Hartenberg Representation

The first step for the modelling of the robot is by using the Denavit-Hartenberg representation [8], a commonly used convention for selecting frames of reference in robotic applications. Each homogenous transformation A_{n+1} is represented as a product of four basic transformations [10], which could be simplified as per Eq.3.1. Each joint of the robot is assigned its respective frame of its revolute joint starting from the base of the robot, which means from joint 1 to joint for this 6-DOF robot to be noted as 0 to 5. Referring to Figure 3.10, Z_0 is assigned at joint 1 representing its rotation, with X_o is parallel to the x-axis of reference frame. Then, Z_1 is assigned at joint 2, with X_1 is in the direction of normal to Z_0 and Z_1 because the two axes are overlapping with each other. This principle of intersecting axes and common normal direction is applied for other joints as well which resulted as in the figure.

$$A_{n+1} = \begin{bmatrix} c\theta_{n+1} & -s\theta_{n+1}c\alpha_{n+1} & s\theta_{n+1}s\alpha_{n+1} & a_{n+1}c\theta_{n+1} \\ s\theta_{n+1} & c\theta_{n+1}c\alpha_{n+1} & -c\theta_{n+1}s\alpha_{n+1} & a_{n+1}s\theta_{n+1} \\ 0 & s\alpha_{n+1} & c\alpha_{n+1} & d_{n+1} \\ 0 & 0 & 0 & 1 \end{bmatrix} \quad \text{(Eq. 3.1)}$$

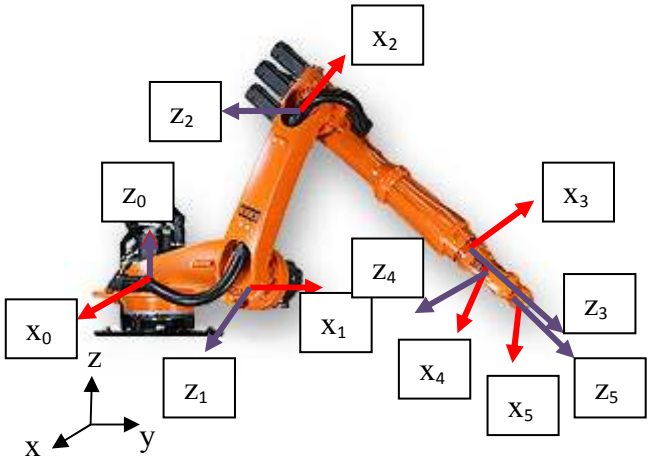

Figure 3.10: Representation of Axes at Each Joint

After the joint axes have been successfully represented, the next step is to construct a parameter table of θ, d, a and α, which is the joint angle, link offset, link length and link twist respectively [10]. The angle 'θ' is defined as angle between two successive x-axis, 'd' is the distance between two successive x-axis, 'a' is the distance between two successive z-axis and 'α' is the angle between two successive z-axis. As a result the parameter table has been constructed as in Table 3.1. The notation of each angle and distance must be carefully done to produce the final transformation matrix.

Table 3.1: Parameter Table of Robot Links and Joints

Link	θ	d	a	α
1	θ_1	0	a_1	90
2	θ_2	0	a_2	0
3	θ_3	d_3	0	90
4	θ_4	0	0	-90
5	θ_5	0	0	90
6	θ_6	0	0	0

Then, the transformation matrix of each joint is derived as below:

$$A_1 = \text{Rot}(z, \theta_1).\text{Trans}(z, a_1).\text{Rot}(x, 90) = \begin{bmatrix} c\theta_1 & 0 & s\theta_1 & a_1c\theta_1 \\ s\theta_1 & 0 & -c\theta_1 & a_1s\theta_1 \\ 0 & 1 & 0 & 0 \\ 0 & 0 & 0 & 1 \end{bmatrix}$$

$$A_2 = \text{Rot}(z, \theta_2).\text{Trans}(z, a_2) = \begin{bmatrix} c\theta_2 & -s\theta_2 & 0 & a_2c\theta_2 \\ s\theta_2 & c\theta_2 & 0 & a_2s\theta_2 \\ 0 & 0 & 1 & 0 \\ 0 & 0 & 0 & 1 \end{bmatrix}$$

$$A_3 = \text{Rot}(z, \theta_3).\text{Trans}(x, d_3).\text{Rot}(x, 90) = \begin{bmatrix} c\theta_3 & 0 & s\theta_3 & 0 \\ s\theta_3 & 0 & -c\theta_3 & 0 \\ 0 & 1 & 0 & d_3 \\ 0 & 0 & 0 & 1 \end{bmatrix}$$

$$A_4 = \text{Rot}(z, \theta_4).\text{Rot}(x, -90) = \begin{bmatrix} c\theta_4 & 0 & -s\theta_4 & 0 \\ s\theta_4 & 0 & c\theta_4 & 0 \\ 0 & -1 & 0 & 0 \\ 0 & 0 & 0 & 1 \end{bmatrix}$$

$$A_5 = \text{Rot}(z, \theta_5).\text{Rot}(x, 90) = \begin{bmatrix} c\theta_5 & 0 & s\theta_5 & 0 \\ s\theta_5 & 0 & -c\theta_5 & 0 \\ 0 & 1 & 0 & 0 \\ 0 & 0 & 0 & 1 \end{bmatrix}$$

$$A_6 = \text{Rot}(z, \theta_6) = \begin{bmatrix} c\theta_6 & -s\theta_6 & 0 & 0 \\ s\theta_6 & c\theta_6 & 0 & 0 \\ 0 & 0 & 1 & 0 \\ 0 & 0 & 0 & 1 \end{bmatrix} \quad \text{(Eq. 3.2)}$$

With transformation matrices of each individual joint found, it is desired to determine the total transformation from the robot base to the end-effector for the usage of calculations in forward and inverse kinematics in the further parts of this report. The total transformation matrix, ${}^{R}T_{E}$, is defined as below:

$${}^{R}T_{E} = A_1A_2A_3A_4A_5A_6 = \begin{bmatrix} n_x & o_x & a_x & P_x \\ n_y & o_y & a_y & P_y \\ n_z & o_z & a_z & P_z \\ 0 & 0 & 0 & 1 \end{bmatrix} \quad \text{(Eq. 3.3)}$$

where:

$n_x = C_1[C_{23}(C_4C_5C_6-S_4S_6)-S_{23}S_5C_6]+S_1(S_4C_5C_6+C_4S_6)$

$n_y = S_1[C_{23}(C_4C_5C_6-S_4S_6)-S_{23}S_5C_6]-C_1(S_4C_5C_6+C_4S_6)$

$n_z = S_{23}(C_4C_5C_6-S_4S_6)+C_{23}S_5C_6$

$o_x = C_1[-C_{23}(C_4C_5C_6+S_4C_6)-S_{23}S_5S_6]+S_1(-S_4S_5S_6+C_4C_6)$

$o_y = S_1[-C_{23}(C_4C_5C_6+S_4C_6)-S_{23}S_5S_6]-C_1(-S_4S_5S_6+C_4C_6)$

$o_z = -S_{23}(C_4C_5C_6+S_4C_6)-C_{23}S_5S_6$

$a_x = C_1[C_{23}C_4S_5+S_{23}C_5]-C_1S_4S_5$

$a_y = S_1[C_{23}C_4S_5+S_{23}C_5]-C_1S_4S_5$

$a_z = S_{23}C_4S_5-C_{23}C_5$

$P_x = C_1(C_2a_2+a_1)+S_1d_3$

$P_y = S_1(C_2a_2+a_1)-C_1d_3$

$P_z = S_2a_2$

3.4 Forward Kinematics Analysis

The next step of the analysis is using the forward kinematics approach to find the resultant transformation matrix at each point given the type of coordinate motion such as Cartesian, spherical, cylindrical or articulated. The derivation of matrix is different for every type where the Cartesian is the simplest compared to articulated motion. For this project, only Cartesian movement is used to make the matrices as simple as possible for this initial stage.

3.4.1 Case Study 1: Horizontal Fuel-Filling Valve Position

For this situation, there are six points of movement need to be analyzed. As mentioned before, these points are pre-determined according to feasible condition in order to simulate the environment.

3.4.1.1 Positioning at P1

This point is the starting point of the end-effector, P, which is defined to be positioned -1.13m in x-axis, 0.7m in y-axis and 0.2m in z-axis from the world reference frame which is considered at the base of the robot.

$$P = \begin{bmatrix} 1 & 0 & 0 & -1.13 \\ 0 & 1 & 0 & 0.7 \\ 0 & 0 & 1 & 0.2 \\ 0 & 0 & 0 & 1 \end{bmatrix}$$

3.4.1.2 Analysis at P2

From P1 to P2, the robot moves in Cartesian coordinate movement at 0.33m along x-axis, 0.3m along y-axis and -0.5m along z-axis, which is noted as ${}^{1}T_{2}$. The updated transformation matrix from P1 to P2 is the product of P and ${}^{1}T_{2}$.

$$ {}^{1}T_{2} = \begin{bmatrix} 1 & 0 & 0 & 0.33 \\ 0 & 1 & 0 & 0.3 \\ 0 & 0 & 1 & -0.5 \\ 0 & 0 & 0 & 1 \end{bmatrix} $$

$$ {}^{0}T_{2} = \begin{bmatrix} 1 & 0 & 0 & -1.13 \\ 0 & 1 & 0 & 0.7 \\ 0 & 0 & 1 & 0.2 \\ 0 & 0 & 0 & 1 \end{bmatrix} \begin{bmatrix} 1 & 0 & 0 & 0.33 \\ 0 & 1 & 0 & 0.3 \\ 0 & 0 & 1 & -0.5 \\ 0 & 0 & 0 & 1 \end{bmatrix} = \begin{bmatrix} 1 & 0 & 0 & -0.8 \\ 0 & 1 & 0 & 1 \\ 0 & 0 & 1 & -0.3 \\ 0 & 0 & 0 & 1 \end{bmatrix} $$

3.4.1.3 Analysis at P3

From P2 to P3, the robot moves in Cartesian coordinate movement at 0.05m along y-axis which is noted as ${}^{2}T_{3}$. The updated transformation matrix from P1 to P3 is the product of ${}^{1}T_{2}$and ${}^{2}T_{3}$.

$$ {}^{2}T_{3} = \begin{bmatrix} 1 & 0 & 0 & 0 \\ 0 & 1 & 0 & 0.05 \\ 0 & 0 & 1 & 0 \\ 0 & 0 & 0 & 1 \end{bmatrix} $$

$$ {}^{0}T_{3} = \begin{bmatrix} 1 & 0 & 0 & -0.8 \\ 0 & 1 & 0 & 1 \\ 0 & 0 & 1 & -0.3 \\ 0 & 0 & 0 & 1 \end{bmatrix} \begin{bmatrix} 1 & 0 & 0 & 0 \\ 0 & 1 & 0 & 0.05 \\ 0 & 0 & 1 & 0 \\ 0 & 0 & 0 & 1 \end{bmatrix} = \begin{bmatrix} 1 & 0 & 0 & -0.8 \\ 0 & 1 & 0 & 1.05 \\ 0 & 0 & 1 & -0.3 \\ 0 & 0 & 0 & 1 \end{bmatrix} $$

3.4.1.4 Analysis at P4

From P3 to P4, the robot moves in Cartesian coordinate movement at -0.05m along z-axis which is noted as ${}^{3}T_{4}$. The updated transformation matrix from P1 to P4 is the product of ${}^{2}T_{3}$ and ${}^{3}T_{4}$.

$$ {}^{3}T_{4} = \begin{bmatrix} 1 & 0 & 0 & 0 \\ 0 & 1 & 0 & 0 \\ 0 & 0 & 1 & -0.05 \\ 0 & 0 & 0 & 1 \end{bmatrix} $$

$$ {}^{0}T_{4} = \begin{bmatrix} 1 & 0 & 0 & -0.8 \\ 0 & 1 & 0 & 1.05 \\ 0 & 0 & 1 & -0.3 \\ 0 & 0 & 0 & 1 \end{bmatrix} \begin{bmatrix} 1 & 0 & 0 & 0 \\ 0 & 1 & 0 & 0 \\ 0 & 0 & 1 & -0.05 \\ 0 & 0 & 0 & 1 \end{bmatrix} = \begin{bmatrix} 1 & 0 & 0 & -0.8 \\ 0 & 1 & 0 & 1.05 \\ 0 & 0 & 1 & -0.35 \\ 0 & 0 & 0 & 1 \end{bmatrix} $$

3.4.1.5 Analysis at P5

From P4 to P5, the robot moves in Cartesian coordinate movement at 0.07m along z-axis which is noted as ${}^{4}T_{5}$. The updated transformation matrix from P1 to P5 is the product of ${}^{3}T_{4}$ and ${}^{4}T_{5}$.

$$ {}^{4}T_{5} = \begin{bmatrix} 1 & 0 & 0 & 0 \\ 0 & 1 & 0 & 0 \\ 0 & 0 & 1 & 0.07 \\ 0 & 0 & 0 & 1 \end{bmatrix} $$

$$ {}^{0}T_{5} = \begin{bmatrix} 1 & 0 & 0 & -0.8 \\ 0 & 1 & 0 & 1.05 \\ 0 & 0 & 1 & -0.35 \\ 0 & 0 & 0 & 1 \end{bmatrix} \begin{bmatrix} 1 & 0 & 0 & 0 \\ 0 & 1 & 0 & 0 \\ 0 & 0 & 1 & 0.07 \\ 0 & 0 & 0 & 1 \end{bmatrix} = \begin{bmatrix} 1 & 0 & 0 & -0.8 \\ 0 & 1 & 0 & 1.05 \\ 0 & 0 & 1 & -0.28 \\ 0 & 0 & 0 & 1 \end{bmatrix} $$

3.4.1.6 Analysis at P6

From P5 to P6, the robot moves in Cartesian coordinate movement at -1.05m along y-axis which is noted as ${}^{5}T_{6}$. The final transformation matrix from P1 to P6 is the product of ${}^{4}T_{5}$ and ${}^{5}T_{6}$.

$$ {}^{5}T_{6} = \begin{bmatrix} 1 & 0 & 0 & 0 \\ 0 & 1 & 0 & -1.05 \\ 0 & 0 & 1 & 0 \\ 0 & 0 & 0 & 1 \end{bmatrix} $$

$$ {}^{0}T_{6} = \begin{bmatrix} 1 & 0 & 0 & -0.8 \\ 0 & 1 & 0 & 1.05 \\ 0 & 0 & 1 & -0.28 \\ 0 & 0 & 0 & 1 \end{bmatrix} \begin{bmatrix} 1 & 0 & 0 & 0 \\ 0 & 1 & 0 & -1.05 \\ 0 & 0 & 1 & 0 \\ 0 & 0 & 0 & 1 \end{bmatrix} = \begin{bmatrix} 1 & 0 & 0 & -0.8 \\ 0 & 1 & 0 & 0 \\ 0 & 0 & 1 & -0.28 \\ 0 & 0 & 0 & 1 \end{bmatrix} $$

3.4.2 Case Study 2: Vertical Fuel-Filling Valve Position

For this situation, there are five points of movement need to be analysed. These points are also pre-determined according to feasible condition in order to simulate the environment.

3.4.2.1 Positioning at P1

This point is the same as in Case Study 1, which is considered the starting point of the end-effector for both situation.

$$ P = \begin{bmatrix} 1 & 0 & 0 & -1.13 \\ 0 & 1 & 0 & 0.7 \\ 0 & 0 & 1 & 0.2 \\ 0 & 0 & 0 & 1 \end{bmatrix} $$

3.4.2.2 Analysis at P2

From P1 to P2, the robot moves in Cartesian coordinate movement at 1.73m along x-axis, 0.45m along y-axis and -0.5m along z-axis, which is noted as ${}^{1}T_{2}$. The updated transformation matrix from P1 to P2 is the product of P and ${}^{1}T_{2}$.

$$ {}^{1}T_{2} = \begin{bmatrix} 1 & 0 & 0 & 1.73 \\ 0 & 1 & 0 & 0.45 \\ 0 & 0 & 1 & -0.5 \\ 0 & 0 & 0 & 1 \end{bmatrix} $$

$$ {}^{0}T_{2} = \begin{bmatrix} 1 & 0 & 0 & -1.13 \\ 0 & 1 & 0 & 0.7 \\ 0 & 0 & 1 & 0.2 \\ 0 & 0 & 0 & 1 \end{bmatrix} \begin{bmatrix} 1 & 0 & 0 & 1.73 \\ 0 & 1 & 0 & 0.45 \\ 0 & 0 & 1 & -0.5 \\ 0 & 0 & 0 & 1 \end{bmatrix} = \begin{bmatrix} 1 & 0 & 0 & 0.6 \\ 0 & 1 & 0 & 1.15 \\ 0 & 0 & 1 & -0.3 \\ 0 & 0 & 0 & 1 \end{bmatrix} $$

3.4.2.3 Analysis at P3

From P2 to P3, the robot moves in Cartesian coordinate movement at 0.05m along y-axis which is noted as ${}^{2}T_{3}$. The updated transformation matrix from P1 to P3 is the product of ${}^{1}T_{2}$and ${}^{2}T_{3}$.

$$ {}^{2}T_{3} = \begin{bmatrix} 1 & 0 & 0 & 0 \\ 0 & 1 & 0 & 0.05 \\ 0 & 0 & 1 & 0 \\ 0 & 0 & 0 & 1 \end{bmatrix} $$

$$ {}^{0}T_{3} = \begin{bmatrix} 1 & 0 & 0 & 0.6 \\ 0 & 1 & 0 & 1.15 \\ 0 & 0 & 1 & -0.3 \\ 0 & 0 & 0 & 1 \end{bmatrix} \begin{bmatrix} 1 & 0 & 0 & 0 \\ 0 & 1 & 0 & 0.05 \\ 0 & 0 & 1 & 0 \\ 0 & 0 & 0 & 1 \end{bmatrix} = \begin{bmatrix} 1 & 0 & 0 & 0.6 \\ 0 & 1 & 0 & 1.2 \\ 0 & 0 & 1 & -0.3 \\ 0 & 0 & 0 & 1 \end{bmatrix} $$

3.4.2.4 Analysis at P4

From P3 to P4, the robot moves in Cartesian coordinate movement at -0.1m along y-axis and -0.05m along z-axis which is noted as ${}^{3}T_{4}$. The updated transformation matrix from P1 to P4 is the product of ${}^{2}T_{3}$ and ${}^{3}T_{4}$.

$$ {}^{3}T_{4} = \begin{bmatrix} 1 & 0 & 0 & 0 \\ 0 & 1 & 0 & -0.1 \\ 0 & 0 & 1 & -0.05 \\ 0 & 0 & 0 & 1 \end{bmatrix} $$

$$ {}^{0}T_{4} = \begin{bmatrix} 1 & 0 & 0 & 0.6 \\ 0 & 1 & 0 & 1.2 \\ 0 & 0 & 1 & -0.3 \\ 0 & 0 & 0 & 1 \end{bmatrix} \begin{bmatrix} 1 & 0 & 0 & 0 \\ 0 & 1 & 0 & -0.1 \\ 0 & 0 & 1 & -0.05 \\ 0 & 0 & 0 & 1 \end{bmatrix} = \begin{bmatrix} 1 & 0 & 0 & 0.6 \\ 0 & 1 & 0 & 1.1 \\ 0 & 0 & 1 & -0.35 \\ 0 & 0 & 0 & 1 \end{bmatrix} $$

3.4.2.5 Analysis at P5

From P4 to P5, the robot moves in Cartesian coordinate movement at -1.4m along x-axis, -1.1m along y-axis and 0.07m along z-axis which is noted as ${}^{4}T_{5}$. The updated transformation matrix from P1 to P5 is the product of ${}^{3}T_{4}$ and ${}^{4}T_{5}$.

$$ {}^{4}T_{5} = \begin{bmatrix} 1 & 0 & 0 & -1.4 \\ 0 & 1 & 0 & -1.1 \\ 0 & 0 & 1 & 0.07 \\ 0 & 0 & 0 & 1 \end{bmatrix} $$

$$ {}^{0}T_{5} = \begin{bmatrix} 1 & 0 & 0 & 0.6 \\ 0 & 1 & 0 & 1.1 \\ 0 & 0 & 1 & -0.35 \\ 0 & 0 & 0 & 1 \end{bmatrix} \begin{bmatrix} 1 & 0 & 0 & -1.4 \\ 0 & 1 & 0 & -1.1 \\ 0 & 0 & 1 & 0.07 \\ 0 & 0 & 0 & 1 \end{bmatrix} = \begin{bmatrix} 1 & 0 & 0 & -0.8 \\ 0 & 1 & 0 & 0 \\ 0 & 0 & 1 & -0.28 \\ 0 & 0 & 0 & 1 \end{bmatrix} $$

3.5 Inverse Kinematics Analysis

The inverse kinematics approach is used to find the joint angles when the initial position and final position is known. Therefore, from the transformation matrices derived at each point using forward kinematics previously, the angles could be easily determined. By comparing each matrix with Eq. 3.3, the respective elements of n_x, n_y, n_z, o_x, o_y, o_z, a_x, a_y, a_z, P_x, P_y and P_z could be found and put into Eq. 3.4 to 3.10 to get each joint angle at each point. Beside this, the values of a_1, a_2 and d_3 are essential, which are 0.45m, 0.68m and 0.7m, respectively, which are the actual dimension of the robot link provided by KUKA Robotics GmbH.

$$\theta_2 = Asin\,(P_z/a_z) \quad \text{(Eq. 3.4)}$$

$$\theta_1 = Acos\left[\frac{P_x(a_2c_2+a_1-P_yd_3)}{{P_x}^2+{P_y}^2}\right] \quad \text{(Eq. 3.5)}$$

$$\theta_{23} = Acos\sqrt{\frac{{P_z}^2-{a_2}^2+(P_xC_1+P_yS_1-a_1)^2}{2{P_z}^2}} \quad \text{(Eq. 3.6)}$$

$$\theta_3 = \theta_{23} - \theta_2 \quad \text{(Eq. 3.7)}$$

$$\theta_4 = Atan\left[\frac{a_xS_1+a_yC_1}{a_xC_1C_{23}+a_yS_1S_{23}+a_zS_{23}}\right] \quad \text{(Eq. 3.8)}$$

$$\theta_6 = Atan\left[\frac{o_zC_{23}-o_xC_1S_{23}-o_yS_1S_{23}}{n_xC_1S_{23}+n_yS_1S_{23}-n_zC_{23}}\right] \quad \text{(Eq. 3.9)}$$

$$\theta_5 = -Atan\left[\frac{a_xC_1C_{23}C_4+a_xS_1S_{23}C_4+a_2S_{23}C_4+a_xS_1S_4-a_yC_1S_4}{-a_xS_{23}-a_yS_1S_{23}+a_zC_{23}}\right] \quad \text{(Eq. 3.10)}$$

After thorough calculation has been performed, the values of joint angles are found for both case studies and summarized in Table 3.2 and Table 3.3, for horizontal and vertical valve, respectively.

Table 3.2: Joint Angles for Case Study 1 (Horizontal Valve)

	Joint 1	Joint 2	Joint 3	Joint 4	Joint 5	Joint 6
P1	-12°	17°	0°	0°	0°	0°
P2	-19°	26°	92°	0°	0°	19°
P3	-25°	26°	54°	0°	20°	25°
P4	-26°	31°	57°	0°	18°	26°
P5	-24°	24°	54°	0°	21°	24°
P6	0°	24°	0°	0°	0°	0°

Table 3.3: Joint Angles for Case Study 2 (Vertical Valve)

	Joint 1	Joint 2	Joint 3	Joint 4	Joint 5	Joint 6
P1	-12°	17°	0°	0°	0°	0°
P2	-84°	26°	92°	0°	0°	84°
P3	-83°	26°	74°	0°	36°	83°
P4	-85°	31°	113°	0°	78°	85°
P5	0°	24°	0°	0°	0°	0°

3.6 Trajectory Planning

The main focus of this paper is how the robot moves from one point to another by investigating on the orientation from the starting to the end point. The movement of the robot shall concern on the part of the path must be attained with a specified timing, thus the velocities and accelerations will come into equation. There are several methods that could be used to determine the trajectories, but this paper utilized on third-order polynomial trajectory planning. Using this method, the initial location and orientation of the robot is known by using the results from inverse kinematics, the joint angles at each position are found.

Considering joint 1 of the robot starts at θ_i and ends at θ_f in t seconds from P1 to P2, which is therefore judged as the boundary conditions for the trajectory. The other boundary conditions that could be considered are that the initial and final joint velocities, $\dot{\theta}_i$ and $\dot{\theta}_f$, are zero respectively because of assuming the robot at rest when starting to move and always coming to stop at each desired point, even it is in the short period. Therefore these four boundary conditions are sufficient to solve the four unknowns of the third-order polynomial in the form of this equation:

$$\theta(t) = c_0 + c_1 t + c_2 t^2 + c_3 t^3 \quad \text{(Eq. 3.11)}$$

Also, taking the first derivative of the polynomial will yield:

$$\dot{\theta}(t) = c_1 + 2c_2 t + 3c_3 t^2 \quad \text{(Eq. 3.12)}$$

By substituting the boundary conditions into Eq. 3.11 and 3.12, four equations could be found and solved simultaneously [17], resulting on the values of the constants, c_0, c_1, c_2 and c_3. Then the joint angle at each time interval could be found which is used by the controller to move the joint to the intended points. The extensive calculations and equations for all points in each case study are discussed in next chapter.

3.7 Summary

In this chapter, the methods on how this project is carried out have been presented in detail. The study is divided into two cases which investigated the layout with the fuel-filling valve been located horizontally or vertically at the vehicle. Besides, a 6-DOF robotic arm in KUKA KR16 LR6-2 together with KR C2 controller has been identified as appropriate for this project, and also simulated using KUKA SimPro. The robot has been generally represented in Denavit-Hartenberg in terms of transformation matrix. The forward kinematics approach has been used to transformation matrices at each movement point for each case, which is six and five points, respectively. Then, the inverse kinematics approach is used to find the angles at each joint at each point mentioned before. For case study 1, there are 36 joint angles associated and 30 joint angles for case study 2 as an essential data for next chapter on trajectory analysis using the third-order polynomial trajectory planning approach.

4.0 Results and Discussion

The robot kinematics modelling will be completed by determining the trajectory of each joint at each point of interest at specific timing using third-order polynomial trajectory planning. From the simulation done, the time at each step could be determined. These timing and angles are essential as boundary conditions to derive the equations of trajectory and velocity at each movement. For each case, the calculations are carefully done and respective graphs are plotted.

4.1 Forward and Inverse Kinematics of the Robot

Theoretically, for each movement of the robot from one point to another has been represented by homogeneous transformation matrix determined in Cartesian coordinates. As mentioned before, the forward and inverse kinematics analysis could be used to find the solution for the transformation between the base of the robot and its end-effector depending on the final location of the tool. These kinematics could be simulated using MATLAB software in which the robot movement at each point is plotted. But first the serial link manipulator of the robot must be created using Robotics toolbox determined from D-H representation from last chapter (Table 3.1). The commands in MATLAB for each D-H parameters are as follow:

```
>> L1 = link ([pi/2, 0.45, 0, 0, 0]);
>> L2 = link ([0, 0.68, 0, 0, 0]);
>> L3 = link ([pi/2, 0, 0, 0.7, 0]);
>> L4 = link ([-pi/2, 0, 0, 0, 0]);
>> L5 = link ([pi/2, 0, 0, 0, 0]);
```

```
>> L6 = link ([0, 0, 0, 0, 0]);
>> r = robot({L1,L2,L3,L4,L5,L6},'NGV');
>> drivebot (r)
```

For a 6-DOF robot, 6 links involved noted with L1 through L6 for each link, where the columns represent the link twist (α), link length (a), joint angle (θ), link offset (d) and joint type (σ), for columns 1 to 5, respectively. The value of σ is zero for revolute joint or non-zero for prismatic joint. Then, the robot link model is created as per Figure 4.1.

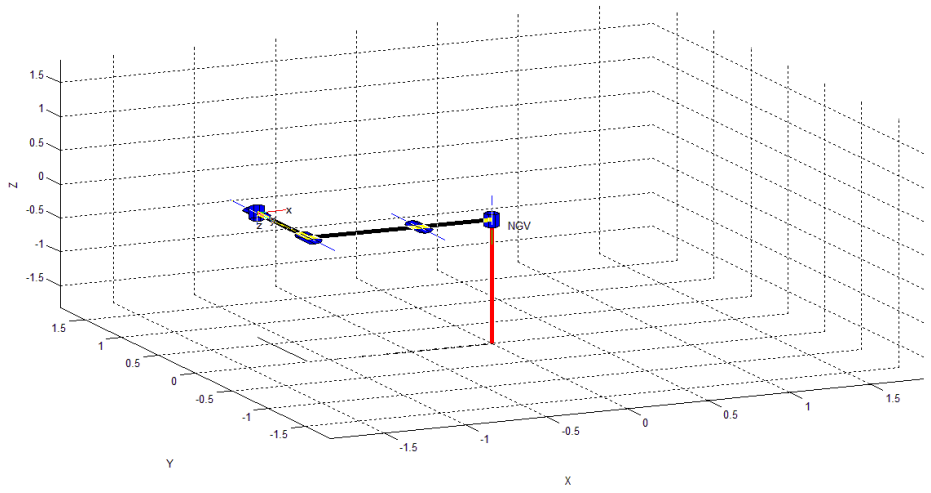

Figure 4.1: Model of six serial links of the robot

After the robot model have been found, the solutions for forward and kinematics analysis for both cases are analyzed using MATLAB using the commands of *fkine* and *ikine* for forward and inverse kinematics respectively. In order to find the solution for each point movement using forward kinematics, usually it is defined by how many degrees that each joint is moving, but in this case, the resultant values from previous chapter will be used because the transformation is defined as in Cartesian when deriving the homogeneous matrix. Taking the example of movement from P1 to P2 for case 1, the robot moves with rotation of -19° for joint 1, 26° for joint 2, 92° for joint 3 and 19° for joint 6. The commands in MATLAB are as follow:

```
>> q12 = [-19*pi/180, 26*pi/180, 92*pi/180, 0, 0,
    19*pi/180]
>> tr12 = fkine (r, q12);
>> drivebot (r, q12)
```

Using the above command, *tr12* will return a value of a '4x4' homogeneous matrix representing the end point orientation and translation of the robot to P2, together with simulation of robot model at P2. The matrix of *tr12* will be displayed as:

```
>> tr12 = fkine (r, q12)
ans =
     1.000         0         0     -0.800
         0     1.000         0     1.000
         0         0     1.000     -0.300
         0         0         0     1.000
```

This result augurs well with the manual derivation of transformation matrix done in previous chapter as it produce very similar result. Then, the steps are repeated for every movement points for each case study 1 and 2. Therefore, the simulation model for each point could be produced as in Figure 4.2 for case study 1 and Figure 4.3 for case study 2. The model also shows how the joints are placed in the space coordinates.

Meanwhile, the *ikine* function is used to determine the joint angles when the transformation matrix already been found. For example, taking the same resultant transformation matrix as before, *tr12*, the commands in MATLAB are as follow:

```
>> qi12 = ikine (r, tr12);
qi12 =
     -0.3317   0.4570    1.6059    0    0    0.3362
```

The results are in the unit of radian and when converted to degrees, it is the same angles calculated using forward kinematics, which have proven the theoretical values.

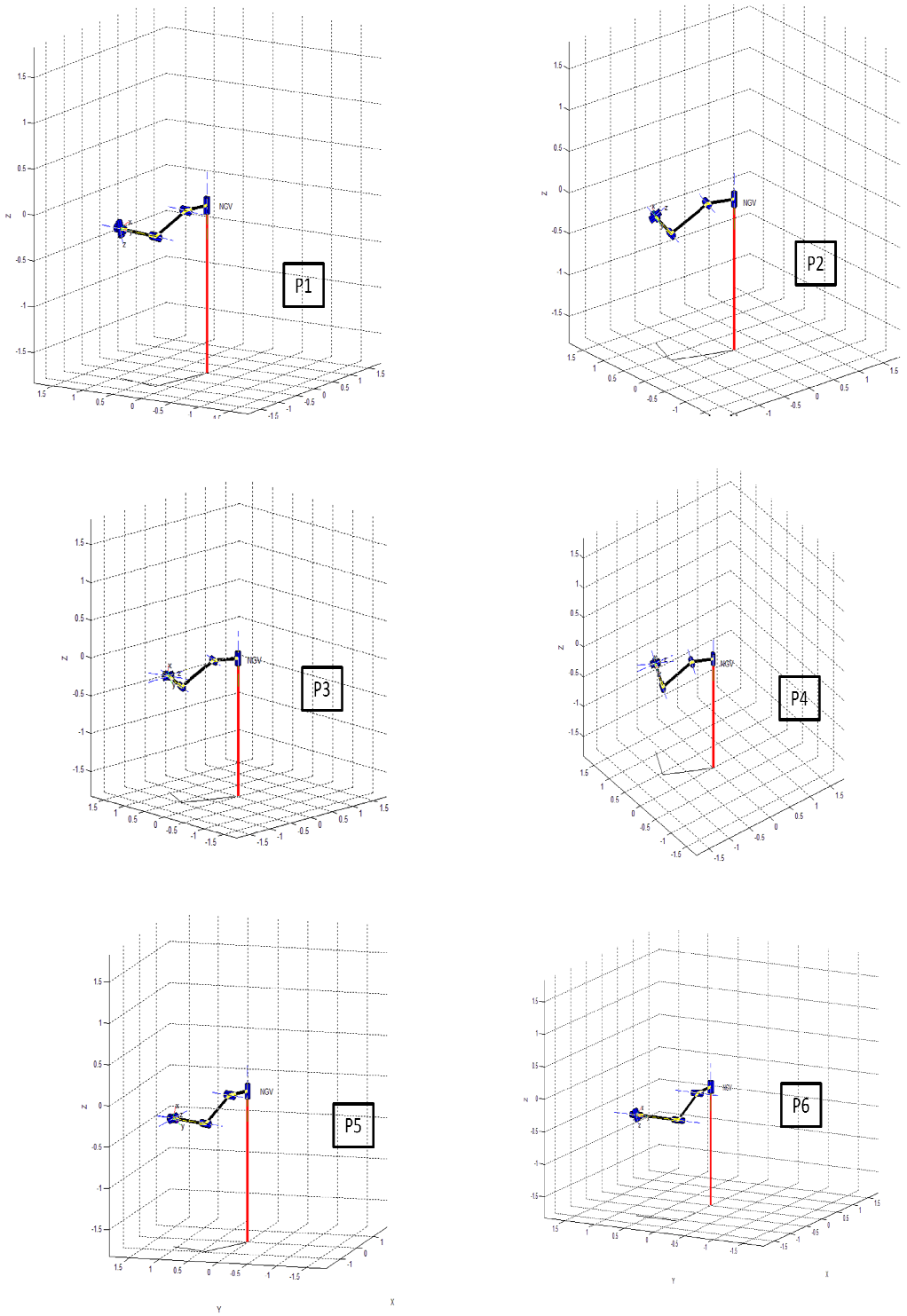

Figure 4.2: Simulation Model for Case Study 1 Using MATLAB

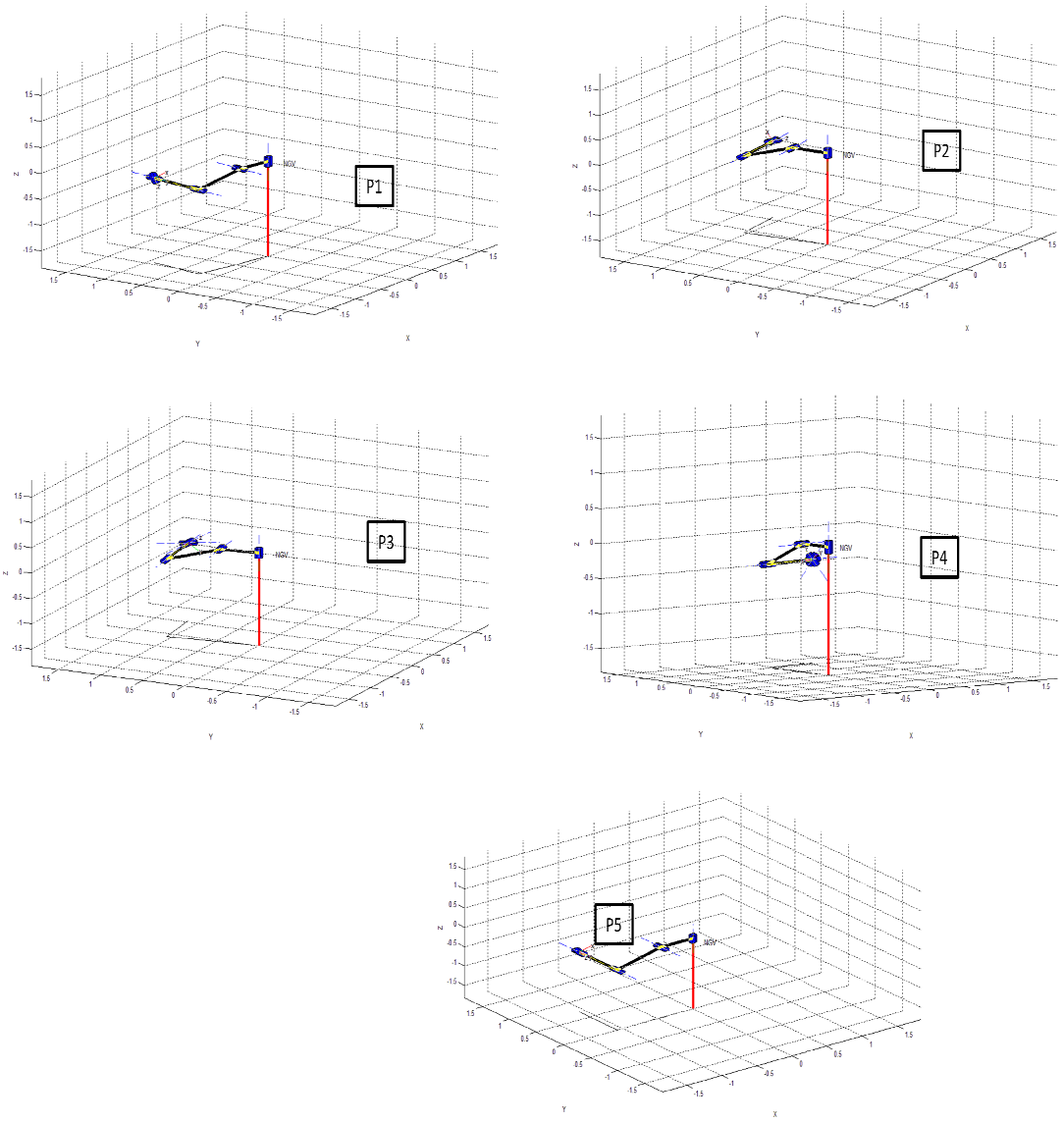

Figure 4.3: Simulation Model for Case Study 2 Using MATLAB

4.2 Trajectory Analysis for Case Study 1 - Horizontal Valve

Using the boundary conditions calculated previously and the time taken, the equations are derived for joint1 and summarized as in Table 4.1. Meanwhile, the graphs of joint angles and velocities are plotted as in Figure 4.4.

Table 4.1: Joint 1 Angles and Velocities Equations - Case Study 1

Robot Movement	Boundary Conditions and Resulting Equations
From P1 to P2	$\theta_i = -12°, \theta_f = -19°, \dot{\theta}_i = \dot{\theta}_f = 0, t = 7.33sec;$ $\theta(t) = -12 - 0.391t^2 + 0.036t^3$ $\dot{\theta}(t) = -0.782t + 0.108t^2$
From P2 to P3	$\theta_i = -19°, \theta_f = -25°, \dot{\theta}_i = \dot{\theta}_f = 0, t = 4.45sec;$ $\theta(t) = -19 - 0.909t^2 + 0.136t^3$ $\dot{\theta}(t) = -1.818t + 0.408t^2$
From P3 to P4	$\theta_i = -25°, \theta_f = -26°, \dot{\theta}_i = \dot{\theta}_f = 0, t = 3.14sec;$ $\theta(t) = -25 - 0.304t^2 + 0.065t^3$ $\dot{\theta}(t) = -0.608t + 0.195t^2$
From P4 to P5	$\theta_i = -26°, \theta_f = -24°, \dot{\theta}_i = \dot{\theta}_f = 0, t = 3.87sec;$ $\theta(t) = -26 + 0.401t^2 - 0.069t^3$ $\dot{\theta}(t) = 0.802t - 0.207t^2$
From P5 to P6	$\theta_i = -24°, \theta_f = 0°, \dot{\theta}_i = \dot{\theta}_f = 0, t = 6.5sec;$ $\theta(t) = -24 + 1.704t^2 - 0.175t^3$ $\dot{\theta}(t) = 3.408t + 0.525t^2$

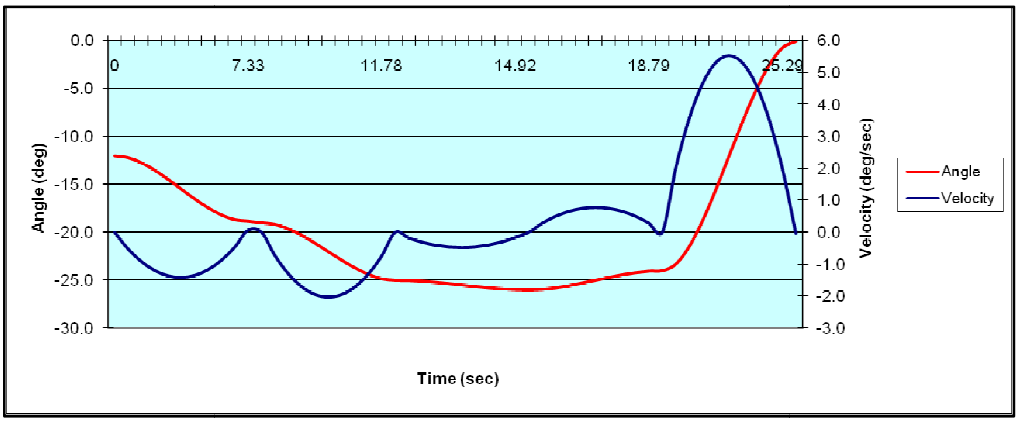

Figure 4.4: Joint 1 Angle and Velocity Graphs - Case Study 1

Referring to the graph, when the robot moves from P1 to P2 in 7.33sec, the angle increase gradually until it reaches -19° measured from the base of the robot. The motor runs from zero to around 1.5 deg/sec in almost 3.5sec before the velocity decrease gradually to zero as it reaches P2. From P2 to P5, the motor moves as the angle increased and only small velocity occurred, even when the filling process occurs at P4. Then, from P5 to P6, the angle is gradually decreasing to 0° while the motor rotates in forward direction with the magnitude of 5.5 deg/sec in 6.5sec.

Table 4.2: Joint 2 Angles and Velocities Equations - Case Study 1

Robot Movement	Boundary Conditions and Resulting Equations
From P1 to P2	$\theta_i = 17°, \theta_f = 26°, \dot{\theta}_i = \dot{\theta}_f = 0, t = 7.33sec;$ $\theta(t) = 17 + 0.503t^2 - 0.046t^3$ $\dot{\theta}(t) = 1.006t + 0.138t^2$
From P2 to P3	$\theta_i = 26°, \theta_f = 26°, \dot{\theta}_i = \dot{\theta}_f = 0, t = 4.45sec;$ $\theta(t) = 26$ $\dot{\theta}(t) = 0$
From P3 to P4	$\theta_i = 26°, \theta_f = 31°, \dot{\theta}_i = \dot{\theta}_f = 0, t = 3.14sec;$ $\theta(t) = 26 + 1.521t^2 - 0.323t^3$ $\dot{\theta}(t) = 3.042t - 0.969t^2$
From P4 to P5	$\theta_i = 31°, \theta_f = 24°, \dot{\theta}_i = \dot{\theta}_f = 0, t = 3.87sec;$ $\theta(t) = 31 - 1.402t^2 + 0.242t^3$ $\dot{\theta}(t) = -2.804t + 0.726t^2$
From P5 to P6	$\theta_i = 24°, \theta_f = 24°, \dot{\theta}_i = \dot{\theta}_f = 0, t = 6.5sec;$ $\theta(t) = 24$ $\dot{\theta}(t) = 0$

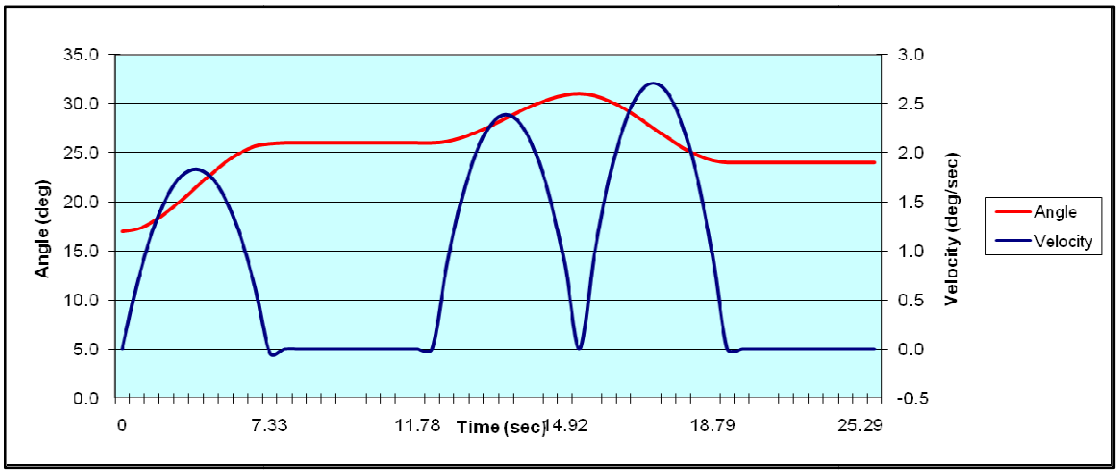

Figure 4.5: Joint 2 Angle and Velocity Graphs - Case Study 1

Moving to joint 2, the equations are summarized in Table 4.2 and the graphs are plotted as in Figure 4.5. The rotation angle starts from 17° to 26° from P1 to P2 in 7.33sec, rotates 5° more to P4 in 7.59sec, and gradually decrease to 24° to P6. While the motor moves in forward direction from P1 to P2, reaching its highest velocity at 1.8 deg/sec, stops at 7.33sec until P3 at 11.78sec before moving again to P4 and in forward direction to P5 before coming to stop until P6.

Table 4.3: Joint 3 Angles and Velocities Equations - Case Study 1

Robot Movement	Boundary Conditions and Resulting Equations
From P1 to P2	$\theta_i = 0°, \theta_f = 92°, \dot{\theta}_i = \dot{\theta}_f = 0, t = 7.33sec;$ $\theta(t) = 5.137t^2 - 0.467t^3$ $\dot{\theta}(t) = 10.274t - 1.311t^2$
From P2 to P3	$\theta_i = 92°, \theta_f = 54°, \dot{\theta}_i = \dot{\theta}_f = 0, t = 4.45sec;$ $\theta(t) = 92 - 5.757t^2 + 0.862t^3$ $\dot{\theta}(t) = -11.514t + 2.586t^2$
From P3 to P4	$\theta_i = 54°, \theta_f = 57°, \dot{\theta}_i = \dot{\theta}_f = 0, t = 3.14sec;$ $\theta(t) = 54 + 0.913t^2 - 0.194t^3$ $\dot{\theta}(t) = 1.826t - 0.582t^2$
From P4 to P5	$\theta_i = 57°, \theta_f = 54°, \dot{\theta}_i = \dot{\theta}_f = 0, t = 3.87sec;$ $\theta(t) = 57 - 0.601t^2 + 0.104t^3$ $\dot{\theta}(t) = -1.202t + 0.312t^2$
From P5 to P6	$\theta_i = 54°, \theta_f = 0°, \dot{\theta}_i = \dot{\theta}_f = 0, t = 6.5sec;$ $\theta(t) = 54 - 3.834t^2 + 0.393t^3$ $\dot{\theta}(t) = -7.668t + 1.179t^2$

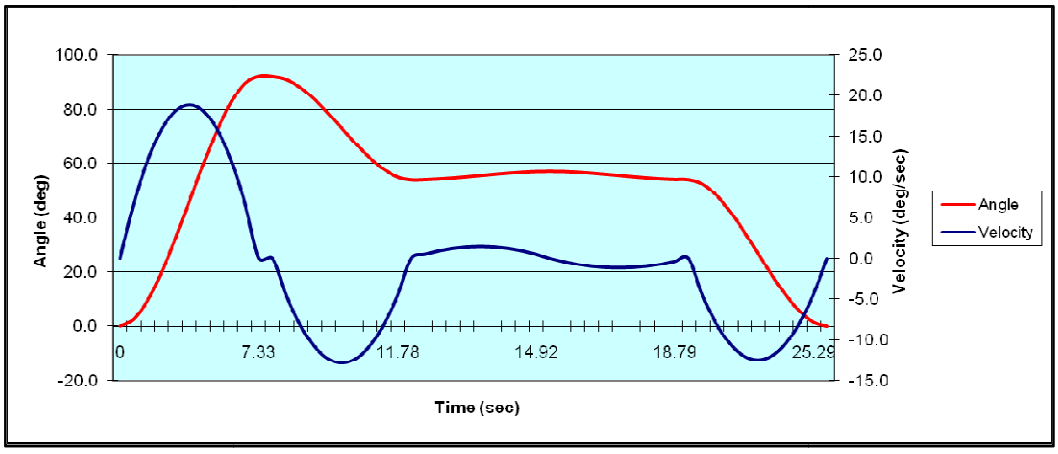

Figure 4.6: Joint 3 Angle and Velocity Graphs - Case Study 1

For joint 3, the equations are summarized in Table 4.3 and the graphs are plotted as in Figure 4.6. The rotation angle starts from 0° to 92° from P1 to P2 in 7.33sec, gradually decrease to 54° at P3 in 4.45sec, increase by 3° to P4 and back to 54° until reaches zero at P6. While the motor moves in forward direction from P1 to P2, reaching its highest velocity at 19 deg/sec, stops at 7.33sec, moves in backward direction until P3 at 11.78sec before moving in low velocity to P5 and in backward direction to stop at P6.

Table 4.4: Joint 5 Angles and Velocities Equations - Case Study 1

Robot Movement	Boundary Conditions and Resulting Equations
From P1 to P2	$\theta_i = 0°, \theta_f = 0°, \dot{\theta}_i = \dot{\theta}_f = 0, t = 7.33sec;$ $\theta(t) = 0$ $\dot{\theta}(t) = 0$
From P2 to P3	$\theta_i = 0°, \theta_f = 20°, \dot{\theta}_i = \dot{\theta}_f = 0, t = 4.45sec;$ $\theta(t) = 3.030t^2 - 0.454t^3$ $\dot{\theta}(t) = -6.060t + 1.362t^2$
From P3 to P4	$\theta_i = 20°, \theta_f = 18°, \dot{\theta}_i = \dot{\theta}_f = 0, t = 3.14sec;$ $\theta(t) = 20 - 0.609t^2 + 0.129t^3$ $\dot{\theta}(t) = -1.218t + 0.387t^2$
From P4 to P5	$\theta_i = 18°, \theta_f = 21°, \dot{\theta}_i = \dot{\theta}_f = 0, t = 3.87sec;$ $\theta(t) = 18 + 0.601t^2 - 0.104t^3$ $\dot{\theta}(t) = 1.202t - 0.312t^2$
From P5 to P6	$\theta_i = 21°, \theta_f = 0°, \dot{\theta}_i = \dot{\theta}_f = 0, t = 6.5sec;$ $\theta(t) = 21 - 1.491t^2 + 0.153t^3$ $\dot{\theta}(t) = -2.982t + 0.459t^2$

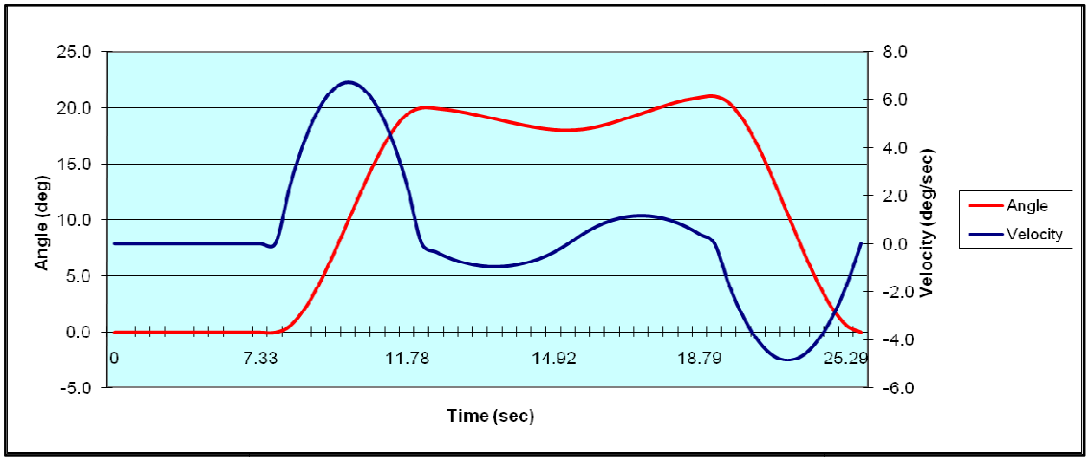

Figure 4.7: Joint 5 Angle and Velocity Graphs - Case Study 1

As for joint 5, the equations are summarized in Table 4.4 and the graphs are plotted as in Figure 4.7. The joint does not move until P2, the rotation angle starts from 0° to 20° from P2 to P3 in 4.45sec, slight rotation of -2° and 3° to P4 and P5 respectively and gradually decrease to 0° at P6 in 6.5sec. While the motor only start to move at P2 in forward direction to P3, reaching its highest velocity at 7 deg/sec, stops at 4.45sec, slight movement of 1.0 deg/sec to P5 in 7.01sec before moving in backward direction to P6 at highest velocity of 5.0 deg/sec before coming to a halt.

Table 4.5: Joint 6 Angles and Velocities Equations - Case Study 1

Robot Movement	Boundary Conditions and Resulting Equations
From P1 to P2	$\theta_i = 0°, \theta_f = 19°, \dot{\theta}_i = \dot{\theta}_f = 0, t = 7.33sec;$ $\theta(t) = 1.061t^2 - 0.096t^3$ $\dot{\theta}(t) = 2.122t - 0.288t^2$
From P2 to P3	$\theta_i = 19°, \theta_f = 25°, \dot{\theta}_i = \dot{\theta}_f = 0, t = 4.45sec;$ $\theta(t) = 19 + 0.909t^2 - 0.136t^3$ $\dot{\theta}(t) = 1.818t - 0.408t^2$
From P3 to P4	$\theta_i = 25°, \theta_f = 26°, \dot{\theta}_i = \dot{\theta}_f = 0, t = 3.14sec;$ $\theta(t) = 25 + 0.304t^2 - 0.065t^3$ $\dot{\theta}(t) = 0.608t - 0.195t^2$
From P4 to P5	$\theta_i = 26°, \theta_f = 24°, \dot{\theta}_i = \dot{\theta}_f = 0, t = 3.87sec;$ $\theta(t) = 26 - 0.401t^2 + 0.069t^3$ $\dot{\theta}(t) = -0.802t + 0.207t^2$
From P5 to P6	$\theta_i = 24°, \theta_f = 0°, \dot{\theta}_i = \dot{\theta}_f = 0, t = 6.5sec;$ $\theta(t) = 24 - 1.704t^2 + 0.175t^3$ $\dot{\theta}(t) = -3.408t + 0.525t^2$

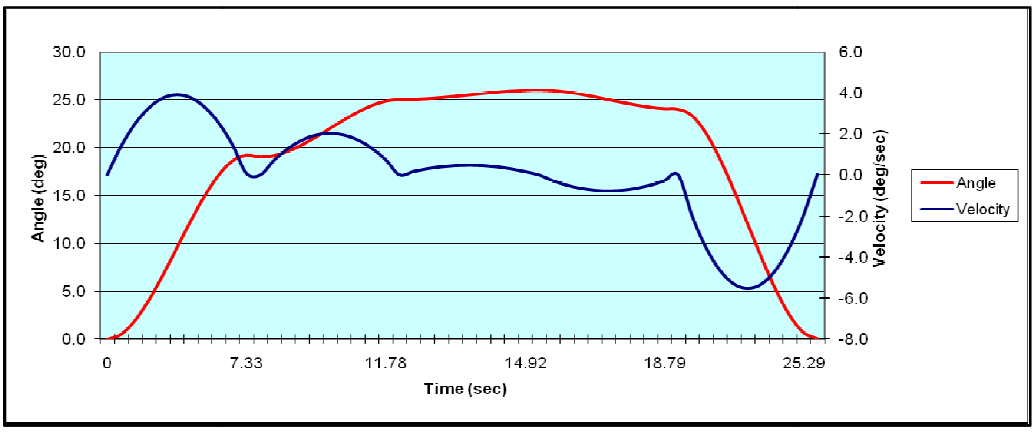

Figure 4.8: Joint 6 Angle and Velocity Graphs - Case Study 1

For joint 6, the equations are summarized in Table 4.5 and the graphs are plotted as in Figure 4.8. The rotation angle starts from 0° to 19° from P1 to P2 in 7.33sec, gradually increase to 25° at P3 in 4.45sec, increase by 1° to P4 and back to 24° until reaches zero at P6. While the motor moves in forward direction from P1 to P2, reaching its highest velocity at 4 deg/sec, stops at 7.33sec, moves at 2.0 deg/sec to P3, moves slowly until P5 in 7.01sec before moving in backward direction to stop at P6.

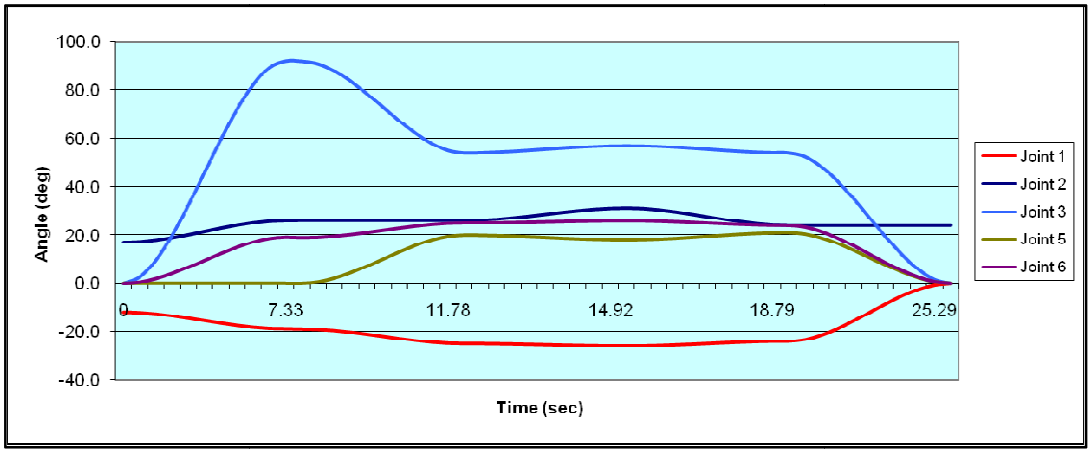

Figure 4.9: Overall Joint Angle and Velocity Graphs - Case Study 1

Lastly, the all graphs are combined to show the overall picture on the trajectory and velocity of robot at each point, as plotted in Figure 4.9. All joints moves in positive angle except joint 1 with the highest movement is through joint 3 which means a large power motor is needed.

4.3 Trajectory Analysis for Case Study 2 - Vertical Valve

The procedure is the same for case study 2. By using the boundary conditions calculated previously and the time taken, the equations are derived for joint 1 and summarized as in Table 4.6. Meanwhile, the graphs of joint angles and velocities are plotted as in Figure 4.10.

Table 4.6: Joint 1 Angles and Velocities Equations - Case Study 2

Robot Movement	Boundary Conditions and Resulting Equations
From P1 to P2	$\theta_i = -12°, \theta_f = -84°, \dot{\theta}_i = \dot{\theta}_f = 0, t = 14.86sec;$ $\theta(t) = -12 - 0.978t^2 + 0.044t^3$ $\dot{\theta}(t) = -1.956t + 0.132t^2$
From P2 to P3	$\theta_i = -84°, \theta_f = -83°, \dot{\theta}_i = \dot{\theta}_f = 0, t = 4.94sec;$ $\theta(t) = -84 + 0.123t^2 - 0.017t^3$ $\dot{\theta}(t) = 0.246t - 0.051t^2$
From P3 to P4	$\theta_i = -83°, \theta_f = -85°, \dot{\theta}_i = \dot{\theta}_f = 0, t = 5.17sec;$ $\theta(t) = -83 - 0.224t^2 + 0.029t^3$ $\dot{\theta}(t) = -0.448t + 0.087t^2$
From P4 to P5	$\theta_i = -85°, \theta_f = 0°, \dot{\theta}_i = \dot{\theta}_f = 0, t = 12.63sec;$ $\theta(t) = -85 + 1.599t^2 - 0.084t^3$ $\dot{\theta}(t) = 3.198t - 0.168t^2$

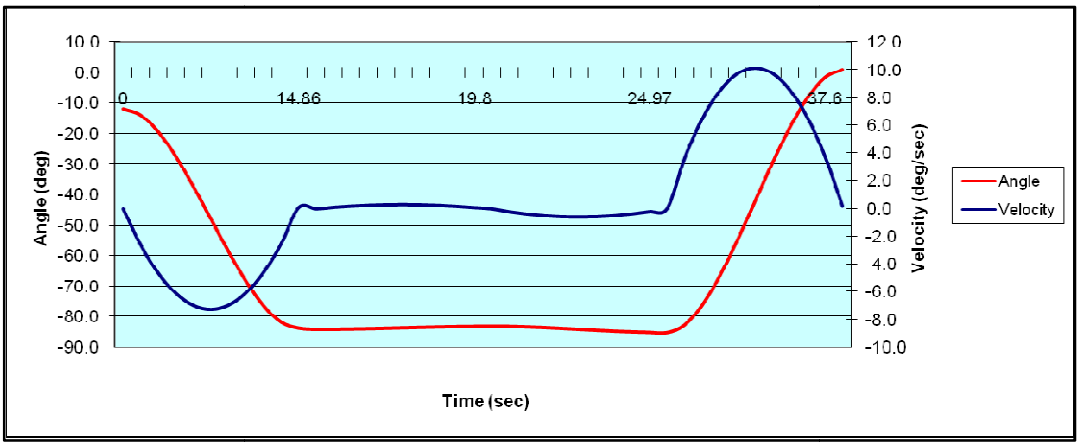

Figure 4.10: Joint 1 Angle and Velocity Graphs - Case Study 2

Referring to the graph, when the robot moves from P1 to P2 in 14.86sec, the angle increase gradually until it reaches -84° measured from the base of the robot. The motor runs from zero to around 8.0 deg/sec in almost 7.5sec before the velocity decrease gradually to zero as it reaches P2. From P2 to P4, the motor almost does not move as the angle and velocity maintained at -84° and 0 deg/sec, respectively, even when the filling process occurs at P3. Then, from P4 to P5, the angle is gradually decreasing to 0° while the motor rotates in backward direction with the magnitude of 10 deg/sec in 12.63sec.

Table 4.7: Joint 2 Angles and Velocities Equations - Case Study 2

Robot Movement	Boundary Conditions and Resulting Equations
From P1 to P2	$\theta_i = 17°, \theta_f = 26°, \dot{\theta}_i = \dot{\theta}_f = 0, t = 14.86sec;$ $\theta(t) = 17 + 0.122t^2 - 0.005t^3$ $\dot{\theta}(t) = 0.244t - 0.015t^2$
From P2 to P3	$\theta_i = 26°, \theta_f = 26°, \dot{\theta}_i = \dot{\theta}_f = 0, t = 4.94sec;$ $\theta(t) = 0$ $\dot{\theta}(t) = 0$
From P3 to P4	$\theta_i = 26°, \theta_f = 31°, \dot{\theta}_i = \dot{\theta}_f = 0, t = 5.17sec;$ $\theta(t) = 26 + 0.561t^2 - 0.072t^3$ $\dot{\theta}(t) = 1.122t - 0.216t^2$
From P4 to P5	$\theta_i = 31°, \theta_f = 24°, \dot{\theta}_i = \dot{\theta}_f = 0, t = 12.63sec;$ $\theta(t) = 31 - 0.132t^2 + 0.007t^3$ $\dot{\theta}(t) = -0.264t + 0.021t^2$

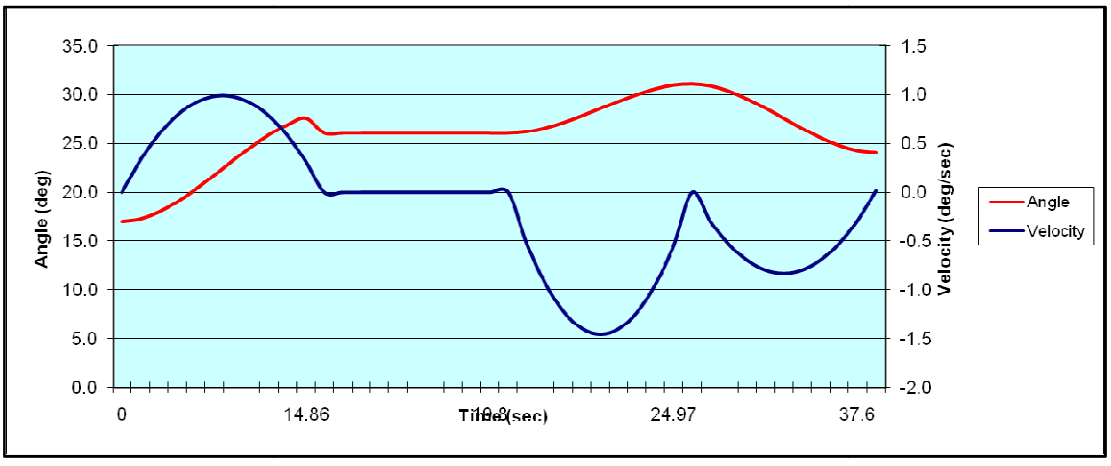

Figure 4.11: Joint 2 Angle and Velocity Graphs - Case Study 2

Moving to joint 2, the equations are summarized in Table 4.7 and the graphs are plotted as in Figure 4.11. The rotation angle starts from 17° to 26° from P1 to P2 in 14.86sec, rotates 5° more to P4 in 10.11sec, and gradually decrease to 24° to P5. While the motor moves in forward direction from P1 to P2, reaching its highest velocity at 1.0 deg/sec, stops at 14.86sec until P3 at 19.8sec before moving again to P4 and in backward direction to P5 before stopping.

Table 4.8: Joint 3 Angles and Velocities Equations - Case Study 2

Robot Movement	Boundary Conditions and Resulting Equations
From P1 to P2	$\theta_i = 0°, \theta_f = 92°, \dot{\theta}_i = \dot{\theta}_f = 0, t = 14.86sec;$ $\theta(t) = 1.250t^2 - 0.056t^3$ $\dot{\theta}(t) = 2.500t - 0.168t^2$
From P2 to P3	$\theta_i = 92°, \theta_f = 74°, \dot{\theta}_i = \dot{\theta}_f = 0, t = 4.94sec;$ $\theta(t) = 92 - 2.123t^2 + 0.299t^3$ $\dot{\theta}(t) = -4.426t + 0.897t^2$
From P3 to P4	$\theta_i = 74°, \theta_f = 113°, \dot{\theta}_i = \dot{\theta}_f = 0, t = 5.17sec;$ $\theta(t) = 74 + 4.377t^2 - 0.564t^3$ $\dot{\theta}(t) = 8.754t - 1.692t^2$
From P4 to P5	$\theta_i = 113°, \theta_f = 0°, \dot{\theta}_i = \dot{\theta}_f = 0, t = 12.63sec;$ $\theta(t) = 113 - 2.125t^2 + 0.112t^3$ $\dot{\theta}(t) = -4.250t + 0.336t^2$

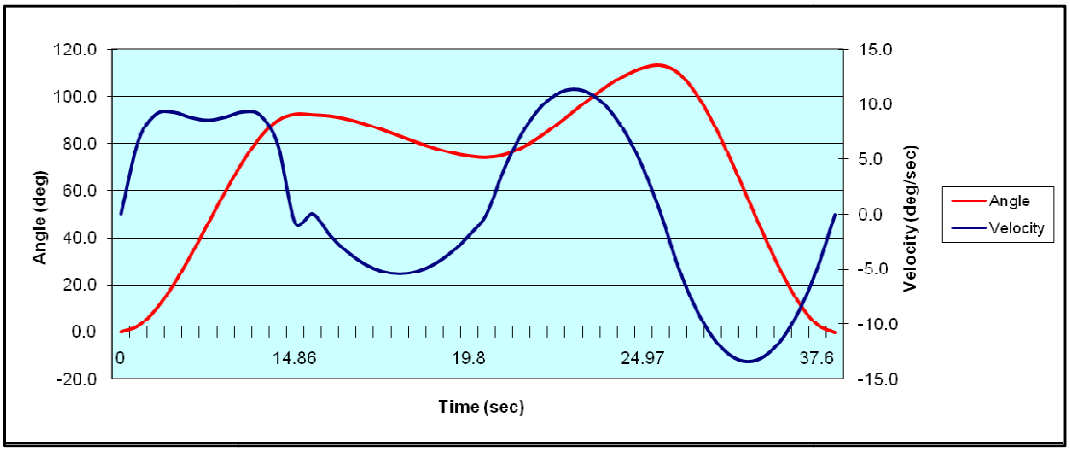

Figure 4.12: Joint 3 Angle and Velocity Graphs - Case Study 2

For joint 3, the equations are summarized in Table 4.8 and the graphs are plotted as in Figure 4.12.The rotation angle starts from 0° to 92° from P1 to P2 in 14.86sec, gradually decrease to 74° at P3 in 4.94sec, increase by 39° to P4 and decreasing until reaches zero at P5. While the motor moves in forward direction from P1 to P2, reaching its highest velocity at 10deg/sec, stops at 14.86sec, moves in backward direction until P3 at 19.8sec, moving in forward direction again to P4 and lastly moves backward direction with its peak of 12.5 deg/sec before stopping at P5.

Table 4.9: Joint 5 Angles and Velocities Equations - Case Study 2

Robot Movement	Boundary Conditions and Resulting Equations
From P1 to P2	$\theta_i = 0°, \theta_f = 0°, \dot{\theta}_i = \dot{\theta}_f = 0, t = 14.86sec;$ $\theta(t) = 0$ $\dot{\theta}(t) = 0$
From P2 to P3	$\theta_i = 0°, \theta_f = -36°, \dot{\theta}_i = \dot{\theta}_f = 0, t = 4.94sec;$ $\theta(t) = -4.426t^2 + 0.597t^3$ $\dot{\theta}(t) = -8.852t + 1.791t^2$
From P3 to P4	$\theta_i = -36°, \theta_f = -78°, \dot{\theta}_i = \dot{\theta}_f = 0, t = 5.17sec;$ $\theta(t) = -36 - 4.714t^2 + 0.608t^3$ $\dot{\theta}(t) = -9.428t + 1.824t^2$
From P4 to P5	$\theta_i = -78°, \theta_f = 0°, \dot{\theta}_i = \dot{\theta}_f = 0, t = 12.63sec;$ $\theta(t) = -78 + 1.467t^2 - 0.077t^3$ $\dot{\theta}(t) = 2.934t - 0.231t^2$

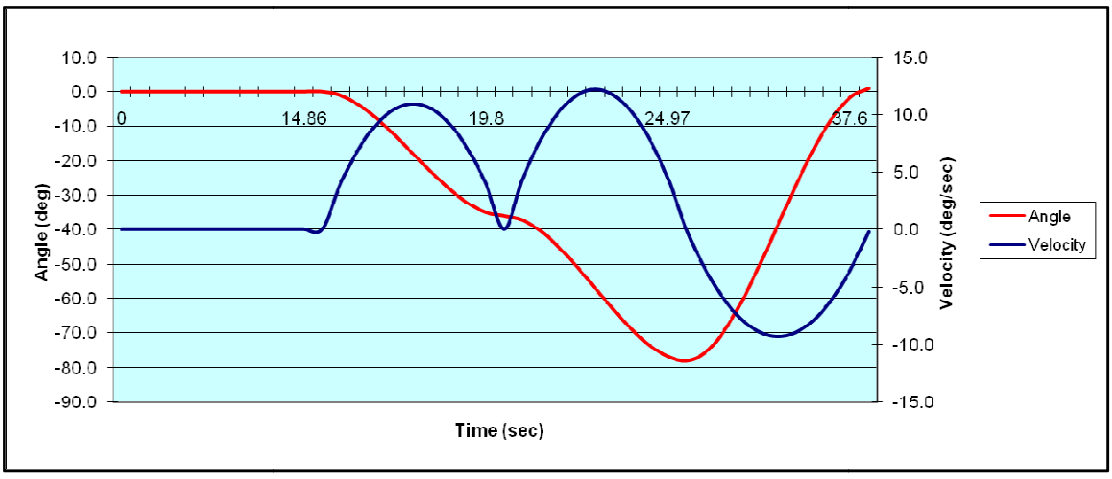

Figure 4.13: Joint 5 Angle and Velocity Graphs - Case Study 2

As for joint 5, the equations are summarized in Table 4.9 and the graphs are plotted as in Figure 4.13.The joint does not move until P2, the rotation angle starts from 0° to -36° from P2 to P3 in 4.94sec, rotates more to -78° at P4 and gradually decrease to 0° at P5 in 12.63sec. While the motor only start to move at P2 in forward direction to P3, reaching its highest velocity at 10 deg/sec, stops after 4.94sec, move forward again in a peak of 12.0 deg/sec to P4 in 5.17sec before moving in backward direction at highest velocity of -10.0 deg/sec before coming to a halt at P5.

Table 4.10: Joint 6 Angles and Velocities Equations - Case Study 2

Robot Movement	Boundary Conditions and Resulting Equations
From P1 to P2	$\theta_i = 0°, \theta_f = 84°, \dot{\theta}_i = \dot{\theta}_f = 0, t = 14.86sec;$ $\theta(t) = 1.141t^2 - 0.051t^3$ $\dot{\theta}(t) = 2.282t - 0.153t^2$
From P2 to P3	$\theta_i = 84°, \theta_f = 83°, \dot{\theta}_i = \dot{\theta}_f = 0, t = 4.94sec;$ $\theta(t) = 84 - 0.123t^2 + 0.017t^3$ $\dot{\theta}(t) = -0.246t + 0.051t^2$
From P3 to P4	$\theta_i = 83°, \theta_f = 85°, \dot{\theta}_i = \dot{\theta}_f = 0, t = 5.17sec;$ $\theta(t) = 83 + 0.224t^2 - 0.029t^3$ $\dot{\theta}(t) = 0.448t - 0.087t^2$
From P4 to P5	$\theta_i = 85°, \theta_f = 0°, \dot{\theta}_i = \dot{\theta}_f = 0, t = 12.63sec;$ $\theta(t) = 85 - 1.599t^2 + 0.084t^3$ $\dot{\theta}(t) = -3.198t + 0.252t^2$

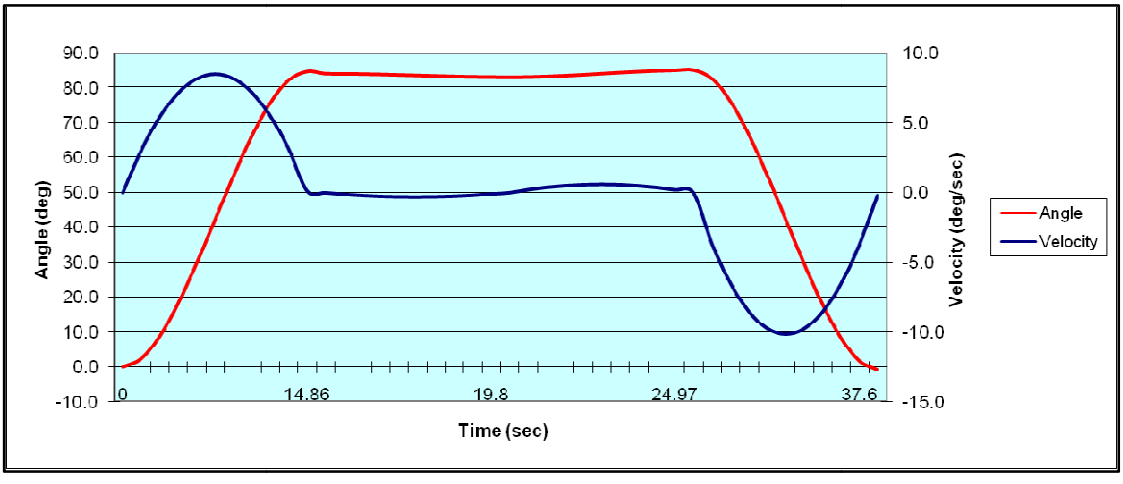

Figure 4.14: Joint 6 Angle and Velocity Graphs - Case Study 2

For joint 6, the equations are summarized in Table 4.10 and the graphs are plotted as in Figure 4.14.When the robot moves from P1 to P2 in 14.86sec, the angle increase gradually until it reaches 84° measured from the base of the robot. The motor runs from zero to around 8.0deg/sec in almost 7.5sec before the velocity decrease gradually to zero as it reaches P2. From P2 to P4, the motor does not move as the angle and velocity maintained at 84° and 0 deg/sec, respectively, even when the filling process occurs at P3. Then, from P4 to P5, the angle is gradually decreasing to 0° while the motor rotates in backward direction with the magnitude of almost the same for movement from P1 to P2 in 12.63sec.

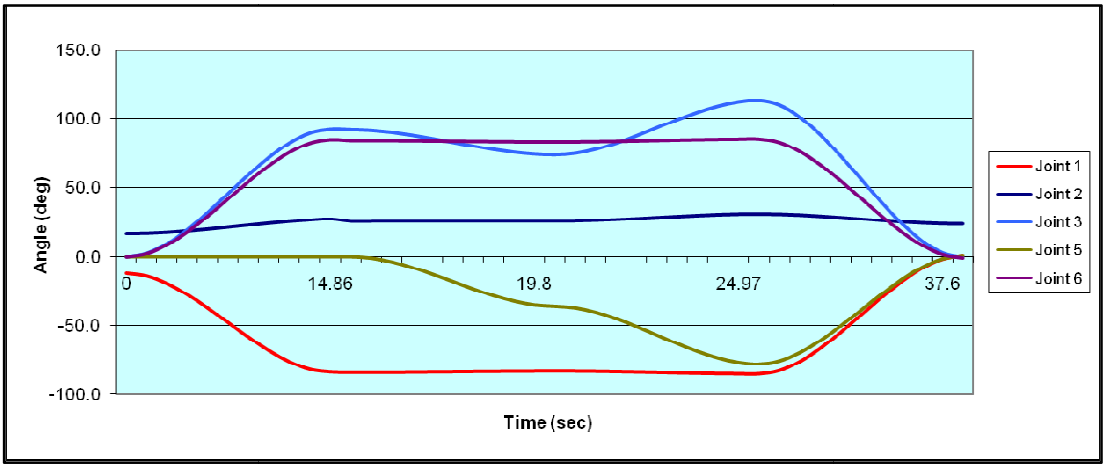

Figure 4.15: Overall Joint Angle and Velocity Graphs - Case Study 2

Lastly, the all graphs are combined to show the overall picture on the trajectory and velocity of robot at each point, as plotted in Figure 4.15. As in case study 1, all joints moves in positive angle except joint 1 and 5 with the highest movement is through joint 1 which means a large power motor is needed. From the graph, it could also be seen that the rotational movement is smooth enough from point to point, with only little disturbance.

4.4 Summary

This chapter discusses the results of forward and inverse kinematics from previous chapter and the simulation model for each cased has been mapped using MATLAB software to show the feasibility of the robot movement. Also, the extensive trajectory analysis of each joint for case study 1 and 2 at all movement points has been examined. The joint angles have been determined using inverse kinematics approach in previous chapter. Once the angles are known, respective equations are found using third-order polynomial trajectory approach in which the general term is:

$$\theta(t) = c_0 + c_1 t + c_2 t^2 + c_3 t^3$$

Each coefficient could be found when the boundary conditions are known. In both cases, the initial and final velocity, $\dot{\theta}_i \; and \; \dot{\theta}_f$, is assumed to be zero at each starting and final point. Meanwhile, the time taken to complete one movement is found when simulated using KUKA SimPro. In case 1, it takes 7.33sec to reach P2 from P1, 4.45sec to reach P3, 3.14sec to reach P4, 3.87sec to reach P5 and 6.5sec to end at P6, while in case 2, 14.86sec is taken from P1 to P2, 4.94sec to P3, 5.17sec to P4 and 12.63sec to stop at P5.

From all the plotted graphs, it is found that the robot has been performing each movement in a controlled way, with the error occurred is minimal. Every rotation of the joint is in the range of valid angle in the robot workspace while the velocity is still considered as optimum even the movement is not much far. It is also could be said that this 6-DOF robot has performed the task in proper orientation even though joint 4 is redundant because the joint does not need to move in this setup. Therefore the trajectory analysis relates to the feasibility of the robot for this application.

5.0 Conclusion

Based on the results provided, the trajectory analysis of robot with application of refuelling natural gas vehicle (NGV) has been successfully performed. The 6-DOF KUKA KR16 L6-2 KS robotic arm could perform the intended task in a pre-determined and fixed layout. A Denavit-Hartenberg convention has been used to generally represent the transformation matrix of the robot has been derived. Two case studies have been investigated depending on the position of the fuel-filling valve and forward kinematics is used to find the transformation matrix at each movement point, which is six and five points for both cases respectively. The robot models for both cases has been simulated using MATLAB to show the joint orientation at each movement point. Then, the joint angles are found using the inverse kinematics approach to be further apply in angles and velocities equations at each joint by implementing the third-order trajectory planning approach. The plotted graphs of the angles and velocities have been analyzed to determine the pattern and feasibility of the movement, discussed in details.

5.1 Recommendations

For future works, it is always a need to design the automatic system in order to detect the position of the valve rather than fixed one. This is very useful as not all vehicles will be very accurate to position their vehicle according to the conditions discussed in this paper. The other essential characteristic to be studied is the obstacle avoidance in order to prevent the robot or human interfering with each other while performing the job. Beside, proper design of nozzle to be attached to the end-effector must also be proposed.

APPENDIX

Appendix A: Individual Points for Trajectory Analysis - Case Study 1

	Joint 1		Joint 2		Joint 3		Joint 4		Joint 5		Joint 6	
	Angle	Velocity	Angle	Velocity	Angle	Velocity	Angle	Velocity	Angle	Velocity	Angle	Velocity
0	-12.0	0.0	17.0	0.0	0.0	0.0	0.0	0.0	0.0	0.0	0.0	0.0
0.733	-12.2	-0.5	17.3	0.7	2.6	6.8	0.0	0.0	0.0	0.0	0.5	1.4
1.466	-12.7	-0.9	17.9	1.2	9.6	12.1	0.0	0.0	0.0	0.0	2.0	2.5
2.199	-13.5	-1.2	18.9	1.5	19.9	15.8	0.0	0.0	0.0	0.0	4.1	3.3
2.932	-14.5	-1.4	20.2	1.8	32.4	18.1	0.0	0.0	0.0	0.0	6.7	3.7
3.665	-15.5	-1.4	21.5	1.8	46.0	18.8	0.0	0.0	0.0	0.0	9.5	3.9
4.398	-16.5	-1.4	22.8	1.8	59.6	18.1	0.0	0.0	0.0	0.0	12.4	3.8
5.131	-17.4	-1.2	24.0	1.5	72.2	15.8	0.0	0.0	0.0	0.0	15.0	3.3
5.864	-18.2	-0.9	25.0	1.2	82.5	12.1	0.0	0.0	0.0	0.0	17.1	2.5
6.597	-18.7	-0.5	25.7	0.6	89.5	6.8	0.0	0.0	0.0	0.0	18.6	1.5
7.33	-18.8	0.1	25.9	0.0	92.1	0.0	0.0	0.0	0.0	0.0	19.2	0.1
7.775	-19.0	0.0	26.0	0.0	92.0	0.0	0.0	0.0	0.0	0.0	19.0	0.0
8.22	-19.2	-0.7	26.0	0.0	90.9	-4.6	0.0	0.0	0.6	2.4	19.2	0.7
8.665	-19.6	-1.3	26.0	0.0	88.0	-8.2	0.0	0.0	2.1	4.3	19.6	1.3
9.11	-20.3	-1.7	26.0	0.0	83.8	-10.8	0.0	0.0	4.3	5.7	20.3	1.7
9.555	-21.1	-1.9	26.0	0.0	78.6	-12.3	0.0	0.0	7.0	6.5	21.1	1.9
10	-22.0	-2.0	26.0	0.0	73.0	-12.8	0.0	0.0	10.0	6.7	22.0	2.0
10.445	-22.9	-1.9	26.0	0.0	67.4	-12.3	0.0	0.0	13.0	6.5	22.9	1.9
10.89	-23.7	-1.7	26.0	0.0	62.2	-10.8	0.0	0.0	15.7	5.7	23.7	1.7
11.335	-24.4	-1.3	26.0	0.0	57.9	-8.2	0.0	0.0	17.9	4.3	24.4	1.3
11.78	-24.8	-0.7	26.0	0.0	55.0	-4.6	0.0	0.0	19.4	2.4	24.8	0.7
12.094	-25.0	0.0	26.0	0.0	54.0	0.0	0.0	0.0	20.0	0.0	25.0	0.0
12.408	-25.0	-0.2	26.1	0.9	54.1	0.5	0.0	0.0	19.9	-0.3	25.0	0.2
12.722	-25.1	-0.3	26.5	1.5	54.3	0.9	0.0	0.0	19.8	-0.6	25.1	0.3
13.036	-25.2	-0.4	27.1	2.0	54.6	1.2	0.0	0.0	19.6	-0.8	25.2	0.4
13.35	-25.4	-0.5	27.8	2.3	55.1	1.4	0.0	0.0	19.3	-0.9	25.4	0.5
13.664	-25.5	-0.5	28.5	2.4	55.5	1.4	0.0	0.0	19.0	-1.0	25.5	0.5
13.978	-25.6	-0.5	29.2	2.3	55.9	1.4	0.0	0.0	18.7	-0.9	25.6	0.5
14.292	-25.8	-0.4	29.9	2.0	56.4	1.2	0.0	0.0	18.4	-0.8	25.8	0.4
14.606	-25.9	-0.3	30.5	1.5	56.7	0.9	0.0	0.0	18.2	-0.6	25.9	0.3
14.92	-26.0	-0.2	30.9	0.9	56.9	0.5	0.0	0.0	18.0	-0.4	26.0	0.2
15.307	-26.0	0.0	31.0	0.0	57.0	0.0	0.0	0.0	18.0	0.0	26.0	0.0
15.694	-25.9	0.3	30.8	1.0	56.9	-0.4	0.0	0.0	18.1	0.4	25.9	-0.3
16.081	-25.8	0.5	30.3	1.7	56.7	-0.7	0.0	0.0	18.3	0.7	25.8	-0.5
16.468	-25.6	0.7	29.5	2.3	56.4	-1.0	0.0	0.0	18.6	1.0	25.6	-0.7
16.855	-25.3	0.7	28.5	2.6	55.9	-1.1	0.0	0.0	19.1	1.1	25.3	-0.7
17.242	-25.0	0.8	27.5	2.7	55.5	-1.2	0.0	0.0	19.5	1.2	25.0	-0.8
17.629	-24.7	0.7	26.5	2.6	55.1	-1.1	0.0	0.0	19.9	1.1	24.7	-0.7
18.016	-24.4	0.7	25.5	2.3	54.7	-1.0	0.0	0.0	20.3	1.0	24.4	-0.7
18.403	-24.2	0.5	24.7	1.7	54.3	-0.7	0.0	0.0	20.7	0.7	24.2	-0.5
18.79	-24.1	0.3	24.2	1.0	54.1	-0.4	0.0	0.0	20.9	0.4	24.1	-0.3
19.44	-24.0	0.0	24.0	0.0	54.0	0.0	0.0	0.0	21.0	0.0	24.0	0.0
20.09	-23.3	2.0	24.0	0.0	52.5	-4.5	0.0	0.0	20.4	-1.7	23.3	-2.0
20.74	-21.5	3.5	24.0	0.0	48.4	-8.0	0.0	0.0	18.8	-3.1	21.5	-3.5
21.39	-18.8	4.6	24.0	0.0	42.3	-10.5	0.0	0.0	16.5	-4.1	18.8	-4.6
22.04	-15.6	5.3	24.0	0.0	35.0	-12.0	0.0	0.0	13.6	-4.7	15.6	-5.3
22.69	-12.0	5.5	24.0	0.0	27.0	-12.5	0.0	0.0	10.5	-4.8	12.0	-5.5
23.34	-8.5	5.3	24.0	0.0	19.0	-12.0	0.0	0.0	7.4	-4.6	8.5	-5.3
23.99	-5.2	4.6	24.0	0.0	11.6	-10.5	0.0	0.0	4.5	-4.1	5.2	-4.6
24.64	-2.5	3.5	24.0	0.0	5.6	-8.0	0.0	0.0	2.2	-3.1	2.5	-3.5
25.29	-0.7	2.0	24.0	0.0	1.5	-4.5	0.0	0.0	0.6	-1.7	0.7	-2.0
25.94	-0.1	0.0	24.0	0.0	-0.1	0.0	0.0	0.0	0.0	0.0	0.1	0.0

Appendix B: Individual Points for Trajectory Analysis - Case Study 2

	Joint 1		Joint 2		Joint 3		Joint 4		Joint 5		Joint 6	
	Angle	Velocity	Angle	Velocity	Angle	Velocity	Angle	Velocity	Angle	Velocity	Angle	Velocity
0	-12.0	0.0	17.0	0.0	0.0	0.0	0.0	0.0	0.0	0.0	0.0	0.0
1.486	-14.0	-2.6	17.3	0.3	2.6	-7.7	0.0	0.0	0.0	0.0	2.4	3.1
2.972	-19.5	-4.6	17.9	0.6	9.6	-15.2	0.0	0.0	0.0	0.0	8.7	5.4
4.458	-27.5	-6.1	19.0	0.8	19.9	-21.5	0.0	0.0	0.0	0.0	18.2	7.1
5.944	-37.3	-7.0	20.3	0.9	32.4	-25.6	0.0	0.0	0.0	0.0	29.6	8.2
7.43	-47.9	-7.2	21.7	1.0	46.0	-26.9	0.0	0.0	0.0	0.0	42.1	8.5
8.916	-58.6	-6.9	23.2	1.0	59.7	-25.5	0.0	0.0	0.0	0.0	54.6	8.2
10.402	-68.3	-6.1	24.6	0.9	72.2	-21.3	0.0	0.0	0.0	0.0	66.1	7.2
11.888	-76.3	-4.6	25.8	0.8	82.6	-15.0	0.0	0.0	0.0	0.0	75.6	5.5
13.374	-81.7	-2.5	26.9	0.6	89.6	-7.5	0.0	0.0	0.0	0.0	82.1	3.2
14.86	-83.6	0.1	27.5	0.3	92.3	0.2	0.0	0.0	0.0	0.0	84.6	0.1
15.354	-84.0	0.0	26.0	0.0	92.0	0.0	0.0	0.0	0.0	0.0	84.0	0.0
15.848	-84.0	0.1	26.0	0.0	91.5	-2.0	0.0	0.0	-1.0	3.9	84.0	-0.1
16.342	-83.9	0.2	26.0	0.0	90.1	-3.5	0.0	0.0	-3.7	7.0	83.9	-0.2
16.836	-83.8	0.3	26.0	0.0	88.1	-4.6	0.0	0.0	-7.8	9.2	83.8	-0.3
17.33	-83.7	0.3	26.0	0.0	85.7	-5.2	0.0	0.0	-12.7	10.5	83.7	-0.3
17.824	-83.5	0.3	26.0	0.0	83.0	-5.5	0.0	0.0	-18.0	10.9	83.5	-0.3
18.318	-83.4	0.3	26.0	0.0	80.3	-5.2	0.0	0.0	-23.3	10.5	83.4	-0.3
18.812	-83.2	0.2	26.0	0.0	77.9	-4.6	0.0	0.0	-28.2	9.2	83.2	-0.2
19.306	-83.1	0.2	26.0	0.0	75.9	-3.5	0.0	0.0	-32.3	7.0	83.1	-0.2
19.8	-83.1	0.1	26.0	0.0	74.5	-1.9	0.0	0.0	-35.0	4.0	83.1	-0.1
20.317	-83.0	0.0	26.0	0.0	74.0	0.0	0.0	0.0	-36.0	0.0	83.0	0.0
20.834	-83.1	-0.2	26.1	-0.5	75.1	4.1	0.0	0.0	-37.2	4.4	83.1	0.2
21.351	-83.2	-0.4	26.5	-0.9	78.1	7.2	0.0	0.0	-40.4	7.8	83.2	0.4
21.868	-83.4	-0.5	27.1	-1.2	82.4	9.5	0.0	0.0	-45.1	10.2	83.4	0.5
22.385	-83.7	-0.6	27.8	-1.4	87.7	10.9	0.0	0.0	-50.8	11.7	83.7	0.6
22.902	-84.0	-0.6	28.5	-1.5	93.5	11.3	0.0	0.0	-57.0	12.2	84.0	0.6
23.419	-84.3	-0.6	29.2	-1.4	99.3	10.9	0.0	0.0	-63.2	11.7	84.3	0.6
23.936	-84.6	-0.5	29.9	-1.2	104.6	9.5	0.0	0.0	-68.9	10.2	84.6	0.5
24.453	-84.8	-0.4	30.5	-0.9	109.0	7.3	0.0	0.0	-73.6	7.8	84.8	0.4
24.97	-84.9	-0.2	30.9	-0.5	111.9	4.1	0.0	0.0	-76.8	4.4	84.9	0.2
26.233	-85.0	0.0	31.0	0.0	113.0	0.0	0.0	0.0	-78.0	0.0	85.0	0.0
27.496	-82.6	3.6	30.8	-0.3	109.8	-4.8	0.0	0.0	-75.8	-3.3	82.6	-3.6
28.759	-76.2	6.5	30.3	-0.5	101.2	-8.6	0.0	0.0	-69.9	-5.9	76.2	-6.5
30.022	-66.6	8.5	29.5	-0.7	88.6	-11.3	0.0	0.0	-61.1	-7.8	66.6	-8.5
31.285	-55.0	9.7	28.5	-0.8	73.2	-12.9	0.0	0.0	-50.5	-8.9	55.0	-9.7
32.548	-42.4	10.1	27.5	-0.8	56.5	-13.4	0.0	0.0	-38.9	-9.3	42.4	-10.1
33.811	-29.7	9.8	26.5	-0.8	39.7	-12.9	0.0	0.0	-27.3	-9.0	29.7	-9.8
35.074	-18.1	8.6	25.5	-0.7	24.3	-11.3	0.0	0.0	-16.5	-7.9	18.1	-8.6
36.337	-8.4	6.6	24.7	-0.5	11.6	-8.6	0.0	0.0	-7.7	-6.1	8.4	-6.6
37.6	-1.8	3.8	24.2	-0.3	2.9	-4.9	0.0	0.0	-1.5	-3.5	1.8	-3.8
38.863	0.8	0.2	24.0	0.0	-0.3	-0.1	0.0	0.0	0.9	-0.2	-0.8	-0.2

BIBLIOGRAPHY

[1] B. Favre-Bulle, "Robot Motion Trajectory - Measurement with Linear Inertial Sensors", Cutting Edge Robotics, 2005, pp. 115-132

[2] B. Shaoping, M.R. Hansen, "Forward Kinematics of Spherical Parallel Manipulators with Revolute Joints", *IEEE/ASME International Conference on Advanced Intelligent Mechatronics, 2008,* 2008, pp. 522-527

[3] CNG-NGV Cylinder, NGV Malaysia. [Online]. Available: http://www.malaysiangv.com/mobstat.html

[4] G. Xiaoqing, W. Jidong, "Trajectory Planning Theory and Method of Industrial Robot", *3rd International Conference on Computer Research and Development, 2011*, 2011, pp. 340-343

[5] Gas Attendant Robot Takes First Step Towards Refueling Satellites in Space. [Online]. Available: http://techland.time.com/2012/03/14/gas-attendant-robot-takes-first-step-towards-refueling-satellites-in-space/

[6] Greenfield Compression Introduction and Component Cost of CNG. [Online]. Available: http://zeitenergy.com/presos/Hightower.pdf

[7] HowStuffWorks "How Natural-gas Vehicles Work". [Online]. Available: http://auto.howstuffworks.com/fuel-efficiency/alternative-fuels/ngv.htm

[8] J. Denavit, R. S Hartenberg, "A Kinematic Notation for Lower-Pair Mechanisms Based on Matrices", **Journal of Applied Mechanics***,* Vol., 1, 1955, pp. 215-221

[9] M.R. Werpy, D. Santini, *et al.*, "Natural Gas Vehicles: Status, Barriers and Opportunities", for Center of Transportation Research Energy Systems Division, Argonne National Library, 2010

[10] M. Dahari, J-D. Tan, "Forward and Inverse Kinematics Model for Robotic Welding Process Using KR-16KS KUKA Robot", *4th International Conference of Modeling, Simulation and Applied Optimization, 2011,* 2011, pp. 1-6.

[11] Natural Gas Vehicle (Wikipedia). [Online]. Available: http://en.wikipedia.org/wiki/Natural_gas_vehicle

[12] NGVs Make The Grade, Natural Gas Vehicles for America. [Online]. Available: http://www.ngvc.org/pdfs/marketplace/SchoolTransportNews_Aug2010.pdf

[13] Q. Qingwen, W. Jixiang, *et al.*, "Trajectory Planning of a 6-DOF Robot Based on RBF Neural Networks", *IEEE International Conference on Robotics and Biomimetics, 2007*, 2007, pp. 324-329

[14] S. Kucuk, Z. Bingul, "Robot Kinematics: Forward and Inverse Kinematics", Industrial Robotics-Theory-Modeling Control, 2006, pp.117

[15] Service Robot (Wikipedia). [Online]. Available: http://en.wikipedia.org/wiki/Service_robot

[16] T. Balkan, M.K. Ozgoren, *et al.*, "Structure-Based Classification and Kinematics Analysis of Six-Joint Industrial Robotics Manipulators", 2006, pp. 964

[17] T. Niemueller and S. Widyadharma, "*Artificial Intelligence – An Introduction to Robotics*", RWTH Aachen, 2003

[18] Technology Assessment of Refuelling-Connection Devices for CNG, LNG and Propane. [Online]. Available: http://gulliver.trb.org/publications/tcrp/tcrp_rrd_25.pdf

[19] Y. Kuriyama, K. Yano, *et al.*, "Trajectory Planning for Meal Assist Robot Considering Spilling Avoidance", *IEEE International Conference on Control Applications, 2008,* 2008, pp. 1220-1225

[20] Y-J. Nam, M-K. Park, "Forward Kinematics of Casing Oscillator", IEEE/ASME Transactions on Mechatronics, Vol. 11, Issue 5, pp. 644-647, 2006